UNIVERSITY OF CALIFORNIA SAN DIEGO

Parvalbumin-positive inhibitory interneuron density in the amygdala in Williams syndrome

A thesis submitted in partial satisfaction of the requirements
for the degree Master of Science

in

Biology

by

Demi Maria Zabala Greiner

Committee in charge:

Katerina Semendeferi, Chair
Brenda Bloodgood, Co-Chair
Stephanie Mel

2019

The thesis of Demi Maria Zabala Greiner is approved, and it is acceptable in quality and form for publication on microfilm and electronically:

_____

_____
Co-Chair

_____
Chair

University of California San Diego

2019

DEDICATION

I would like to dedicate my thesis to the best supporters one can ask for: my parents and brother. Without their sacrifice, dedication, and love, I would not have been given the opportunity for higher education, let alone completing a master's degree in science. They are my strength and have encouraged me to follow my dreams. I only hope to spread the energy they give me to others and my future endeavors.

TABLE OF CONTENTS

ACKNOWLEDGEMENTS

I have been a member of the Laboratory for Human Comparative Neuroanatomy for over three years where I began my journey to becoming the scientist I am today. My research experience has been predominantly led by female scientists, which is an incredibly inspiring and rare privilege that I hope to embody and portray in my all future endeavors. I would like to thank Professor Katerina Semendeferi for her insightful commentary not only in courses and throughout the drafting of this thesis, but for advice in being a confident scientist. I would like to thank Dr. Caroline Lew and Dr. Kari Hanson for being incredible mentors not only for my master's thesis research, but for helping me navigate through life's many twists and turns. I would like to thank my fellow research assistants Kimberly Groeniger and Deion Cuevas for the years of support, friendship, and encouragement making my experience in neuroanatomy research that much more incredible. I would like to thank graduate students, Branka Hrvoj and Linnea Wilder, for their constructive input and advice throughout my time in this lab. I would like to thank my committee members, Professor Brenda Bloodgood and Professor Stephanie Mel, for their support and being incredible role models through our courses together and mentorship. Lastly, I would like to thank the donors and family of the donors of the material used in this study. Our work would not be possible without the generous, courageous act of tissue donation for scientific inquiry.

Chapter 1 includes material currently being prepared for submission for publication in a peer-reviewed journal. Greiner, Demi Maria Z.; Lew, Caroline H.; Hanson, Kari L.; Cuevas, Deion; Groeniger, Kim M.; Semendeferi, Katerina. Parvalbumin-positive inhibitory interneuron density in the amygdala in Williams syndrome. The thesis author was the primary investigator of this material in this master's thesis.

ABSTRACT OF THE THESIS

Parvalbumin-positive inhibitory interneuron density in the amygdala in Williams syndrome

by

Demi Maria Zabala Greiner

Master of Science in Biology

University of California San Diego, 2019

Professor Katerina Semendeferi, Chair
Professor Brenda Bloodgood, Co-Chair

Williams syndrome (WS) is a rare neurodevelopmental disorder caused by a microdeletion in chromosomal region 7q11.23 affecting approximately 25-28 genes. Individuals with this disorder display a unique hypersocial phenotype involving a seemingly uninhibited social approach, alongside several physiological and intellectual impairments. Many studies have characterized the genetic and behavioral phenotype of WS, however due to WS infrequency, there is limited research on how the genetic deletion affects neuroanatomical structure. The

amygdala is a brain structure pivotal for the regulation of social and emotional behavior. Disruptions to the inhibitory interneuron system within the amygdala have been documented in other neurodevelopmental disorders, but not yet examined in WS. Through unbiased stereological and immunohistochemical approach, parvalbumin-positive (PV+) inhibitory interneuron density was measured within the lateral, basal, accessory basal and central nuclei of the amygdala in four *post mortem* human brains of individuals with WS and four matched controls. There was no significant difference of PV+ inhibitory interneuron density in WS compared to neurotypical controls in all amygdaloid nuclei. However, for both groups, the lateral nucleus demonstrated a regional specialization of PV+ interneurons not seen in the other nuclei examined. This is the first study to quantify GABAergic inhibitory interneuron density within the amygdala of WS individuals and one of a handful of studies to quantify interneuron density in the human brain. This study contributes important findings for future research that aim to examine neuronal mechanisms within WS and other neurological disorders involving atypical social behaviors in which inhibitory circuitry may be affected.

INTRODUCTION

Chapter 1 has been prepared as the future peer-reviewed publication of this study. It was designed first with a concise background section, followed by materials and methods, results, and discussion. This study explores the inhibitory interneuron system within an important brain structure in the context of a rare neurodevelopmental disorder, Williams syndrome.

Chapter 2 contains extensive background information of this study, including detailed explanations of its unique aspects explored including Williams syndrome, the amygdala, and the GABAergic inhibitory system within the brain. This chapter is meant to provide ample detail on the specific aspects of the study, essentially an extension to the background from Chapter 1.

Chapter 3 includes concluding statements denoting the significance of the present study. The nature of Williams syndrome, human *post mortem* tissue, and inhibitory network research individually is uncommon, but together, even more so. In turn, this represents the novelty and value of the present study's unique elements.

CHAPTER 1: PARVALBUMIN-POSITIVE INHIBITORY INTERNEURON DENSITY IN THE AMYGDALA WILLIAMS SYNDROME

Background

Williams syndrome (WS) is a rare neurodevelopmental disorder caused by a hemizygous deletion in chromosomal region 7q11.23 resulting in a distinctive hypersocial phenotype alongside several physiological impairments and intellectual modulations (Doyle, Bellugi, Korenberg, & Graham, 2004; Korenberg et al., 2000). The mechanisms underlying these somatic physical phenotype of WS is well-characterized; however, while genes in the WS deletion such as GTF2IRD1, CYCLN2, and LIMK1 have been implicated in social cognition, emotional behavior (particularly fear), and neuronal development (Arber et al., 1998; Donnai & Karmiloff-Smith, 2000; Porter et al., 2012; Serrano-Juárez et al., 2018; van Hagen et al., 2007; Young et al., 2008), little is known about the neuroanatomical correlates of the distinct hypersocial phenotype. Williams syndrome poses a unique opportunity to study known genetic deletions that result in a characteristic, consistent social phenotype and many studies have been conducted in unraveling WS at the genetic and behavioral levels (Martens, Wilson, & Reutens, 2008). What is rather lacking in research is the bridge between the two levels: the affected anatomy, particularly the brain microstructure. The neurological underpinnings of the hypersocial phenotype is not well-understood and examining the microstructure of brain regions linked to sociobehavioral circuitry are critical in bridging the gap between genotype, neuroanatomy, and behavior.

The amygdala is a subcortical structure located in the medial-temporal lobe and is typically known as pivotal region for emotional information processing, especially fear (Davis, 1992; Ochsner & Gross, 2005). Additionally, the amygdala has been characterized in the "social brain" (Brothers, 1990), serving as a central point for the convergence of social and emotional

sensory information (Adolphs 2003; Klüver and Bucy 1939; Murray 2007). There are 13 distinct amygdaloid nuclei, each defined by neuronal morphology, electrophysiology, function, and/or connectivity to other brain regions (Sah et al. 2003). The four nuclei in the amygdala commonly examined and distinguished in this study include the lateral, basal, accessory basal (together referred to as the basolateral nucleus) and the central nucleus, because of their defined morphological boundaries compared to other nuclei and unique connectivity with brain regions (Stefanacci & Amaral, 2000, 2002). Each nucleus has an important role in the relay of sensory information to many cortical and subcortical regions, as well as integrating that information between the nuclei (Sah et al. 2003). Generally, the basolateral nuclei relay information to and from higher-order cognitive areas, such as the orbitofrontal and prefrontal cortices, sensory cortices, and subcortical structures like hippocampal associated areas (Stefanacci & Amaral, 2000). The central nucleus receives major projections from the basolateral nucleus and subsequently projects to autonomic structures in the brainstem (Stefanacci & Amaral, 2002). The amygdala has demonstrated microstructural modulation in WS such as increased overall volume (Jernigan and Bellugi 1990; Reiss et al. 2000) and increased overall and lateral nucleus density (Lew et al. 2018), as well as other neurodevelopmental disorders including autism spectrum disorders (ASD) and schizophrenia (Amaral, Schumann, & Nordahl, 2008; Kreczmanski et al., 2007).

The main population of amygdaloid neurons are glutamatergic excitatory principal neurons, comprising approximately 80-90% of total neurons (McDonald & Augustine, 1993; Pitkänen & Amaral, 1994). The remaining are mainly local γ-aminobutyric acid containing, or GABAergic, inhibitory interneurons that regulate the glutamatergic excitatory principal neuron activity (McDonald & Augustine, 1993). A well-characterized subpopulation of GABAergic

interneurons is immunopositive for the neuronal protein, parvalbumin or PV+. PV+ interneurons make up 19-43% of the total GABAergic interneuron population, alongside other inhibitory interneuron subtypes including calbindin and calretinin (McDonald & Mascagni 2001). GABAergic PV+ interneurons function to control the excitability of single principal neurons and other interneurons, as well as synchronizing the frequency of groups of principal neurons (Cobb, Buhl, Halasy, Paulsen, & Somogyi, 1995; Spampanato, Polepalli, & Sah, 2011; Woodruff, Monyer, & Sah, 2006; Woodruff & Sah, 2007b). Due to PV+ interneurons' role in the direct regulation of excitatory activity within the amygdala (Spampanato et al., 2011; Woodruff & Sah, 2007a), it is possible that PV+ interneuron density alteration can cause improper amygdala function. Inhibitory interneuron dysfunction has been implicated in several neurological disorders that include atypical mental and behavioral phenotypes, such as ASD, schizophrenia, and Fragile X syndrome (Berretta, Pantazopoulos, & Lange, 2007; Coghlan et al., 2012a; Prager, Bergstrom, Wynn, & Braga, 2016; Schumann, Bauman, & Amaral, 2011).

Given the critical role of the amygdala in social behavior, WS's unique hypersocial drive, and the role of the inhibitory interneuron system in modulating neuronal circuitry, the inhibitory regulation of the amygdala of WS is a potential site of dysfunction. This pilot study is the first to measure an important inhibitory interneuron population within the amygdala of WS individuals. Utilizing immunohistochemical and unbiased stereological techniques, the PV+ interneuron density was measured in four nuclei of the amygdala in *post mortem* tissue of four WS and age-, sex-, and hemisphere-matched control pairs. I hypothesized that the seemingly uninhibited hypersocial WS phenotype may be the result of a higher PV+ inhibitory interneuron density with the amygdala, a highly innervated socio-emotional processing area of the brain, due to the greater inhibitory regulation neurons that would be present. With greater inhibitory interneuron

presence, I hypothesize that there would be greater inhibition of the fear/threat detection ability of the amygdala reflected in a "fearless" social approach, such as the WS social phenotype.

Materials and Methods

(Initials Key for Research Scientists and Research Assistants: KS = Dr. Katerina Semendeferi, CL = Dr. Caroline Lew, KH = Dr. Kari Hanson, DC = Deion Cuevas, KG = Kimberly Groeniger, DG = Demi Greiner)

Subjects

Post mortem brain tissue of the amygdala from four Williams syndrome brains and four neurotypical, or control, age-, sex-, and hemisphere-matched brains were used in this study (Table 1). Brain tissue of Williams syndrome individuals were received from the Ursula Bellugi Brain Collection and neurotypical brain tissue was received from the NIH NeuroBioBank. All amygdala brain blocks were formalin-fixed and subsequently saturated in a series of sucrose solutions prior to cutting for optimal cutting condition and cryoprotection. Amygdala tissue blocks were frozen on dry ice and sectioned in a 1-in-5 series at 80 µm thickness via microtome by CL, KG, and DG (Leica SM 2010R). One series per subject was mounted on gelatin-coated glass slides and stained for Nissl substance, and the remaining were stored in tissue cryopreservation solution (TCS) and kept at -20°C prior to immunohistochemical staining. The selection of tissue sections for immunohistochemical staining spans the rostral-caudal extent of the amygdala in each individual in a 1-in-20 series.

Immunohistochemistry

The immunohistochemical tissue processing was carried out by DG with the assistance of KH, CL, DC, and KG. All amygdala tissue sections were processed by immunohistochemical staining for the neuronal marker parvalbumin. After each step in this tissue staining process such as washes and solution incubation, the tissue-filled plates were placed on an orbital shaker table (KJ 210BD Oscillator) at 80 rotations per minute to maximize tissue contact with the surrounding solution. Frozen tissues submerged in TCS were defrosted and washed in phosphate buffer solution B (PBS-B). Antigen retrieval was performed by submerging tissue in 0.5% citraconic acid in deionized water solution (pH = 7.4), heated at 86°C for 30 minutes, cooled, then washed in PBS-B. The tissue was quenched for endogenous peroxidases with a 3% hydrogen peroxide-methanol solution incubated for 20 minutes, then washed in PBS-B. Pre-block solution was prepared using 4% normal serum, 0.6% Triton-X, 5% BSA in PBS-B and incubated with the tissues for 1 hour, then washed in PBS-B. Mouse primary antibody (#235, SWAnt; Marly, Switzerland) in PBS-B at 1:8000 concentration was applied to tissues and incubated for 24 hours at room temperature, then 24 hours at 4°C. The tissue was then washed and incubated with anti-mouse secondary antibody (BA-2000, Vector Laboratories, Inc., Burlingame, CA) in PBS-B at 1:200 concentration for 1 hour at room temperature. The tissue was then washed in PBS-B and the avidin-biotin peroxidase complex (ABC) kit (PK-4000, Vector Laboratories, Inc.; Burlingame, CA) was incubated with the tissue for 1 hour at room temperature, then washed with PBS-B. The DAB (3,3'-diaminobenzidine) chromogen kit (SK-4100, Vector Laboratories, Inc.; Burlingame, CA) was prepared according to the manufacturer's instructions. DAB solution containing double-distilled water, buffer stock solution, DAB stock solution, and hydrogen peroxide and was incubated with the tissue shaking for a maximum of 8

minutes until desired dark brown color was obtained. After desired darkly stained color was achieved, the tissues were transferred to PSB-B to halt the reaction and the tissues were mounted onto gelatin coated slides (#5075-W, Brain Research Laboratories; Newton, MA). After the immunostained tissue had dried onto the slides, the slides were dehydrated in a gradient of ethanol solutions then transferred into Citrisolv (Decon Laboratories, Inc.; King of Prussia, PA). Glass coverslips were applied onto the tissue by DG, DC, and KG using Permount (Fisher Scientific; Pittsburgh, PA) as adhesive medium. The slides were then dried overnight before quantitative stereology and microscopy.

Stereological Analysis

Stereological analysis of the tissue was performed by DG with the guidance of KH and CL. Unbiased designed-based stereological analysis of the immunostained tissue was performed using a Nikon Eclipse 80i brightfield microscope and the Optical Fractionator probe of Stereoinvestigator software (MBF Bioscience; Williston, VT). The Optical Fractionator probe allows for the estimation of a total population of cells based on random sampling within outlined regions of interest on sections spanning a uniform z-plane. Each subject had 5-9 amygdala tissue sections to quantify spanning the rostral-caudal extent of the structure. Boundaries of each the four nuclei were drawn in reference to the adjacent Nissl stained sections from the same subject at 1x magnification consistent with previously published amygdala boundaries (Schumann & Amaral, 2005). The grid size per nucleus was optimized to take into consideration the less abundant interneuron population compared to total neuron population and to be proportional to the size of each nuclei: 900 x 900 μm^2 (lateral), 750 x 750 μm^2 (basal), 500 x 500 μm^2 (accessory basal), and 350 x 350 μm^2 (central). Other stereological parameters such as counting frame size

and dissector height remained consistent for all nuclei: 350 x 350 μm^2 and 20 µm, respectively. An example of a single counting site within the program is shown in Figure 1. Neuron soma that were within the counting frame were counted. Neuron soma that lay within the counting frame and intersected green lines were marked, whereas neuron soma that were within the counting frame and intersected the red lines were not marked (Figure 1). Neuron soma that were darkly stained and had neuron-like morphology (processes, clear cell body shape) were counted. A threshold coefficient of error (Gundersen m = 1) was used to monitor and account for the variability of neuron quantification within each subject. For this study, Gundersen CE m = 1 values of < 0.2 calculated for each nucleus per subject were considered reliable, values exceeding 0.2 were not considered reliable for consistent comparison. PV+ interneuron density (neurons/mm^3) was calculated as the estimated population using mean section thickness with counts (neurons) divided by planimetric volume of the structure (mm^3). Other reported measures such as total neuron count during one nuclei probe run and coefficient of error were also included in this study. Total neuron count represents the raw number of neurons measured during each probe run. Estimated total population represents the estimated projection of all interneurons within the entire structure. Volume represents the planimetric volume or the volume calculated based on the boundaries drawn from the serial sections.

Statistical Analysis

All statistical tests were performed on GraphPad Prism Version 8.1.0 for Windows (GraphPad Software, La Jolla, California, USA). A two-way ANOVA was performed to test the variable of condition (WS) and differences between nuclei. Mann-Whitney tests (non-parametric, unpaired t-tests for comparing two groups) were performed following the ANOVA to compare

WS condition within each of the nuclei with a measured Gundersen coefficient of error m = 1 < 0.2, numerical criterion based on a prominent interneuron density study (Kataoka et al., 2010).

Results

This study aimed to measure the parvalbumin-positive interneuron density within four major subdivisions of *post mortem* human amygdala of the Williams syndrome brain. Quantitative stereological results are listed in Table 2, including the estimated total population, volume, total population density, and percentage (%) of total neuron density. The data reveal no significant difference in PV+ interneuron density in Williams syndrome group compared to neurotypical control group across all four amygdaloid nuclei (two-way ANOVA, $p < 0.05$). Figure 2 represents the individual values and group means comparing the WS subjects and their corresponding controls in each nucleus. Figure 3 represents the individual values of WS and neurotypical control pairs within each nucleus. There was a significantly greater PV+ interneuron density between the lateral and central nucleus within the WS group (Freidman test, $p = 0.0370$, not shown), however statistical tests involving the accessory basal and central nuclei were not deemed reliable due to their large coefficients of error (Gundersen m = 1, > 0.2) and large standard deviations. The neurotypical group did not show significant differences of interneuron density between all nuclei, likely due to small sample size.

Figure 4 illustrates the qualitative PV+ interneuron density distribution across the four nuclei distinguished in this study: the lateral, basal, accessory basal, and central nuclei. The rostral-caudal extent of the amygdala was represented across the tissue sections quantified, however the mid-amygdala region was chosen for representation in this figure because of the presence of all four nuclei distinguished in this region of the amygdala. The lateral nucleus had

the greatest PV+ interneuron density for the WS and neurotypical individuals generally, however there was greatest PV+ interneuron density distributed along the most lateral portion of this nucleus. This figure (Figure 4) depicts one section of one subject (WS14) of the study, however this pattern was observed in most other tissue sections per subject. Other nuclei were not observed to have this consistent regionalization, but rather more ubiquitously distributed.

Discussion

Through a neuroanatomical and stereological approach, parvalbumin-positive interneuron density within the four major nuclei of the human amygdala in Williams syndrome individuals was measured. This is the first study quantitatively measuring of the PV+ interneuron density within the WS amygdala.

The PV+ interneurons tightly regulate the activity of excitatory neurons within the major nuclei of the amygdala, part of the fear network of the brain (McDonald & Betette, 2001; Woodruff & Sah, 2007b). A higher inhibitory interneuron density within this structure may disrupt the typical excitatory activity causing an imbalance of excitation/inhibition regulation and improper neural networking (Marín, 2012). Amygdala PV+ interneurons were hypothesized to have higher density in all nuclei within WS compared to neurotypical individuals because of the seemingly uninhibited, “fearless” social drive seen in WS. With a higher density of the subunits of the inhibitory regulation mechanism present, in theory, there would be increased overall inhibition of the structure’s neuronal activity. Particularly for the amygdala, there would be social fear inhibition because of the structure’s important convergence in socio-emotional information processing (Adolphs, 2006; Murray, 2007). The greater inhibitory interneuron

density or inhibitory control may be associated with the lack of social fear inhibition, in other words being prosocial, seen within the WS phenotype.

The results show that there was no significant difference between the WS groups and neurotypical control group across all four of the major amygdaloid nuclei, which does not support the initial hypothesis, but the measurements are similar to previous human interneuron density studies (Pantazopoulos, Lange, Hassinger, & Berretta, 2006; Garcia-Amado and Prensa, 2010). Additionally, only the lateral and basal nucleus measurements were considered reliable due to their acceptable CE during quantification. There are several possible explanations for these results including small sample size, scarce PV+ interneuron numbers leading to large coefficients of error, roles of other inhibitory interneuron populations, and the possibility of a functional difference of the interneurons as opposed to an anatomical difference. Other aspects of this study such as the apparent PV+ interneuron localization within the lateral nucleus, neurotypical subject NT5758, and limitations of the study will be discussed in further detail.

Other Interneurons

Parvalbumin-positive interneurons are one of the main inhibitory interneuron populations in the cortex and the amygdala (Markram et al., 2004; McDonald & Mascagni, 2001). There have been quantitative interneuron studies within the human amygdala, which have served as the basis for this study's observations, however only one study was found to have comparable methodological density units of neurons/mm^3 whereas other studies used neurons/mm^2.

Both parvalbumin and calretinin interneurons were quantified as a percentage out of total neuron density in a cohort of three neurotypical subjects in Garcia-Amado and Prensa (2010). The calretinin-positive interneurons, another major GABAergic inhibitory interneuron

population, had greater density in the four amygdaloid nuclei distinguished in this study compared to the PV+ population, representing 4-23% of the total neuron population whereas PV+ interneurons were <1% of the total neuron (Garcia-Amado and Prensa, 2010). Total neuron counts of individuals from this study were taken from Lew et al. (2018), a study within our laboratory, and the percentage of PV+ interneurons in the total neuron population was calculated. Within this comparison, our results showed that PV+ interneurons also comprised approximately 1% or less of total amygdaloid neuron density, similar to Garcia-Amado and Prensa (2010). Our study contributes to the line of evidence that the PV+ interneuron density is consistently low across the human amygdala, but other interneuron populations may be present in larger numbers.

Pantazopolous et al. (2006) describe quantitative measures of multiple interneuron subpopulations within the human amygdala including parvalbumin-positive (PV+), calbindin-positive (CB+), and parvalbumin/calbindin-positive interneurons (PV/CB+) that demonstrated statistically different number of each neuronal subpopulations in the different nuclei throughout the amygdala. However, the interneuron density measurements were calculated in units of neurons/mm^2, as opposed to this study's density units of neurons/mm^3. Neurons/mm^2 measures the density of neurons within an area on a particular "2D" section, however this study's use of estimated total neuron populations and structure volume estimations in calculating an estimated total neuron number within a cubic (^{3}) volume provides a more accurate measure for density. Therefore, comparisons of interneuron density can be made on a qualitative basis. CB+ interneurons showed greater number ubiquitously throughout the amygdala and particularly in more medial nuclei, like the accessory basal and central domains, whereas the PV+ showed greater number in the rostral/mid-amygdala region and lateral nucleus, similar to the findings of the present study. This again indicates that the PV+ interneurons immunostained represents one

of many subpopulations of GABAergic interneurons and that other subpopulations may be populating and localizing in the other regions.

Sorvari et al. (1995) has also depicted this similar PV+ interneuron pattern in the human amygdala, however density measurements in this study were calculated in neurons/mm^2 which leaves our density comparisons on a qualitative level. Similar PV+, CR+, and CB+ distribution patterns are present in the rat amygdala, where PV+ was more robustly present in the more lateral nuclei and sparse in the medial nuclei. CR+ and CB+ were more evenly distributed throughout all amygdaloid nuclei, notably populating the central nucleus consistent with past studies (Kemppainen & Pitkanen, 2000; McDonald & Betette, 2001). Future studies quantifying all the major GABAergic interneuron subpopulations within the human amygdala for WS may illustrate a more comprehensive overview of the regional specialization of the entire inhibitory interneuron system. The other major interneuron subpopulations may achieve greater statistical power across the amygdaloid nuclei which may provide support for this study's hypothesis that there would be greater inhibitory interneuron density overall within the WS amygdala.

Electrophysiology

PV+ interneurons may not have significantly greater density within the amygdala in WS, but another proposed explanation for this is perhaps an underlying functional mechanism over glutamatergic principal neurons, a feature that neuroanatomical work cannot directly determine. PV+ interneurons have characteristic electrophysiological activity within the basolateral amygdala exhibiting fast-spiking bursts (Rainnie, Mania, Mascagni, & McDonald, 2006; Spampanato et al., 2011) and are involved in feedforward and feedback inhibition and excitation

systems dependent on the type of afferent cell, glutamatergic or interneuron respectively (Woodruff et al., 2006; Woodruff & Sah, 2007a, 2007b).

In ASD, there is a reduction of GABAergic system elements in various cortical regions (Coghlan et al., 2012a). In a Fragile X syndrome model, there is a reduction of GABAergic transmission, inhibitory synapses, and synaptic GABA levels within the amygdala (Olmos-Serrano et al., 2010). Within schizophrenia, there is reduced GABA precursor protein with conserved neuron number in the PFC and cerebellum (Akbarian et al., 1995; Guidotti et al., 2000) and reduced excitation in PV+ interneurons (Belforte et al., 2010). GABAergic dysfunction is slowly being revealed as a common finding in neuropsychiatric and neurological disorders (Coghlan et al., 2012b; Marín, 2012), however many of the research studies involved electrophysiological and protein expression methods contributing insights to the functionality of the interneurons as opposed to its structural differences. Functionality and anatomy are complements of each other, paralleled research of neuroanatomy and electrophysiology for this dichotomy would illustrate the complete role of interneurons in regulatory neurotransmission.

Regional Localization

In this study, I found that the lateral nucleus exhibits higher PV+ interneuron density compared to the other nuclei in both neurotypical and WS human amygdala, although insignificant (Table 2, Figure 4). This distribution pattern has been present in the human amygdala (Garcia-Amado and Prensa, 2010; Pantazopoulos et al., 2006; Sorvari et al., 1995), as well as the monkey (Pitkänen & Amaral, 1993), and rat (Kemppainen & Pitkanen, 2000). The lateral nucleus can be subdivided into two regions in humans: lateral (outer most) and medial (inner most) (Pitkänen & Kemppainen, 2002; Sorvari et al., 1995). As described in the

aforementioned studies, PV+ interneurons populate the basolateral nucleus predominantly compared to other amygdaloid nuclei, especially within the lateral nucleus. Accordingly, within our study, the lateral-most portion of the lateral nucleus, as opposed to the medial subdivision, had the highest PV+ interneuron density in both the WS and neurotypical control groups. This recurrent pattern may provide insight on the specificity of PV+ interneuron information regulation.

The lateral nucleus has unique innervation and circuitry with other parts of the brain, largely from cortical sensory areas (Sah et al. 2003; Stefanacci and Amaral 2002). It is the main information input area of the amygdala and starts the information processing from multimodal sensory areas (Stefanacci & Amaral, 2000). This higher density of a specific inhibitory interneuron type in this particular nucleus may indicate that PV+ interneurons favorably regulate afferent information from mainly sensory territories, as opposed to autonomic territories or other nuclei like such as the central nucleus. In Lew et al. (2018), the lateral nucleus demonstrated an increase to overall neuron density in neurotypical individuals, which may account for this increased overall density of this particular nucleus. The neurodevelopmental trajectory of amygdala neurons has demonstrated a medial to lateral gradient, where neuronal migration begins in the more medial nuclei, like the central nucleus, and end in the lateral nucleus (Kordower, Piecinski, & Rakic, 1992). This pattern may implicate a mechanism that contributes to the uneven distribution of the PV+ interneurons in the mature lateral nucleus.

The human entorhinal cortex and prefrontal cortex also have regional specialization and lamina-specificity, respectively, of inhibitory interneurons subpopulations including PV+ (Lewis et al., 2001; Mikkonen, Soininen, & Pitkänen, 1997). This interneuron type may be suited for regulating specific types of incoming information across the human brain.

NT5758

One subject in the control group, NT5758, demonstrated an unusual staining pattern that greatly differed from all other individuals observed in this study, as well as previous PV+ interneuron studies (Garcia-Amado and Presna, 2010; Kemppainen & Pitkanen, 2000; Pantazopoulos et al., 2006). Of the six amygdala sections quantified for this individual, two sections in the caudal region showed an abnormal staining pattern containing densely packed, darkly stained PV+ soma in the upper portions of the accessory basal and central nuclei. The nuclei boundaries and stained cells were verified for accuracy by two senior lab members.

The causal mechanisms underlying the abnormal PV+ interneuron density observed in subject NT5758 remain elusive. The cause of death for subject NT5758 was sepsis, a condition of extreme organ failure due to a hyperactive host immune response and commonly results in brain cognitive dysfunction (Lever & Mackenzie, 2007; Siami, Annane, & Sharshar, 2008). There is evidence that induced sepsis decreases overall neuron number in the brain, PV+ interneuron function, and cognitive ability in mice, (Ji et al., 2015; Semmler et al., 2007), so it is possible that complications of sepsis contributed to this irregular robust localized staining.

Limitations

Due to the nature of neuroanatomical work for this rare neurodevelopmental disorder, the WS sample size for this pilot study was n = 4. Therefore, conclusions drawn from the data are based on a small subset of WS cases and may not be representative of the entirety of the disorder but do provide the neuroanatomical groundwork for further studies to build upon as well as novel findings. There are two main points of limitation: sample size and low neuron number.

Firstly, the unique intersection of topics this study addresses include a rare neurodevelopmental disorder like Williams syndrome, *post mortem* tissue in humans and quantification of interneurons makes these findings novel, but subject to small sample size. This study contained four WS subjects and four neurotypical control subjects, one of the neurotypical subjects had only the lateral nucleus present. Having very few subjects produces data that may not be fully representative of density measures for each of the groups. By increasing the number of subjects within the study, we can get a more accurate representation of what the density of the PV+ interneuron population more likely is. The low sample size also poses the issue of statistical power and reliability. However, *post mortem* human studies hold valuable information that an animal model or cell culture lack which is the actual human measurement within the species of interest, not an extrapolated or hypothesized one.

Secondly, although interneurons play a critical role in the regulation of neuronal activity in cortical and subcortical structures, they make up a minority of the overall neuron population (DeFelipe, 2002; Markram et al., 2004; Sorvari et al., 1996). This poses the issue of reliable estimation and quantification due to their sparse distribution. Amygdala GABAergic interneurons comprise approximately 10-25% of the total neuron population (McDonald & Augustine, 1993; Pitkänen & Amaral, 1994). When sampling interneurons, let alone a subtype of interneurons, there is a chance for low overall counts that result in high coefficients of error or high probability of inaccuracy.

The Optical Fractionator probe (MBF Bioscience; Williston, VT) used to measure the density of these interneurons in this study operates by estimating the total population of a cell type by randomly sampling on a uniform grid throughout a series of sections expanding the entire extent of the structure. This method of unbiased, design-based stereology allows for a

quantitative estimation of a cell subpopulation, without having to physically count every cell within the structure. A measure of accuracy for this estimation is the coefficient of error (CE), or how largely the cell counts measured in each nucleus per section differ from the average count of that nuclei from all the sections. The more sections there are to quantify, the closer the "true" average value will be, and therefore deviations from the "true" average are less accurate.

The lateral nucleus tended to have the highest overall neuron counts and density as compared to other nuclei in both WS and neurotypical groups (Table 2). Having a larger number of neurons resulted in the lowest coefficients of error compared to the other nuclei due to their consistently higher count throughout a majority of the amygdala (Table 2). The second most PV+ interneuron dense nucleus was the basal nucleus with a corresponding lower density and higher average CE compared to the lateral. Next were the accessory basal and central nuclei, with even lower densities and higher CE's (Table 2). Due to the lower and lower counts overall in particular nuclei, the subsequent CE's were higher, indicating high amounts of variation and deviations from the mean. For instance, in the central nuclei of NT4916 and NT5758 there was only one marked PV+ interneuron within the entire region sampled per subject (Table 2). Other sections contained zero counts, resulting in even greater deviations from the mean and the highest CE measurable, which is 1.0.

Amygdala nuclei density measurements that achieved levels of unreliable coefficients of error, Gundersen CE m =1 > 0.2 or greater than a 20% chance of error, were not considered reliable data. Nuclei per individual that surpassed a CE of 0.2 were not considered in statistical tests or drawing viable conclusions from. This criterion subsequently eliminates reliable quantitative comparisons of the accessory basal and central nuclei in both the WS and neurotypical groups, leaving only the lateral and basal nuclei for quantitative comparison,

statistical analysis, and reliable discussion. Measuring the densities for low-count neuron populations yields an issue of accuracy but may be remedied by increasing the number of measurable sections per nuclei and number of individuals. These territories stained positively for neurotransmitter fibers and positive cells and increasing the number of sections may allow for future quantification of interneuron density in these regions. However, this may not be the best use of this incredibly rare and precious tissue. Due to the rarity of the tissue available, the maximum amount of quantifiable sections was used in this study, 5-9 sections per individual. In future studies, more sections per individual may be added such as using a 1-in-10 series as opposed to this study's 1-in-20 series to lower the CE and to more accurately measure more neuron scarce nuclei.

Conclusion

This is the first study to obtain quantitative measures of an amygdaloid interneuron subpopulation of *post mortem* individuals with Williams syndrome. Preliminary conclusions can be made from the lateral and basal nuclei findings where PV+ interneurons show a regional localization, potentially indicative of incoming sensory information regulation by this cell-type specifically. Williams syndrome subjects tended to follow this pattern of localized PV+ interneuron density within the lateral nucleus, therefore potential modulation in functionality or density changes in other inhibitory interneuron subpopulations within the amygdala may be occurring. While this study did not find significant differences in PV+ interneuron density in WS and neurotypical controls, our findings of very low numbers of PV+ interneurons suggests that subpopulations of other inhibitory interneurons are more prevalent in the amygdala, and thus my hypothesis that greater density throughout all amygdala nuclei in WS cannot be ruled out as a

contributing mechanism explaining the uninhibited social drive phenotype. The underlying evidence suggests that the amygdala, a socially and emotionally implicated brain structure, may have a modulated inhibitory regulation network is apparent due to the known structural change in the WS amygdala and the modulated inhibitory regulation networks in other neurodevelopmental disorders. Williams syndrome demonstrates a consistent genotype-phenotype relationship where its genetic mechanisms result in atypical social behavior that can be further understood by neuroanatomical study in the context of neural network regulation systems.

Chapter 1 includes material currently being prepared for submission for publication in a peer-reviewed journal. Greiner, Demi Maria Z.; Lew, Caroline H.; Hanson, Kari L.; Cuevas, Deion; Groeniger, Kim M.; Semendeferi, Katerina. Parvalbumin-positive inhibitory interneuron density in the amygdala in Williams syndrome. The thesis author was the primary investigator of the material in this master's thesis.

CHAPTER 2: EXTENDED BACKGROUND

Williams Syndrome

Williams syndrome (WS) is a rare neurodevelopmental disorder occurring 1 in 7,500–20,000 births with a uniquely social behavioral phenotype (Morris, Demsey, Leonard, Dilts, & Blackburn, 1988; Strømme, Bjømstad, & Ramstad, 2002). One of the most defining characteristics of WS is "hypersociability", such that WS individuals, compared to typically developing individuals, approach and engage in social interactions in an uninhibited manner, especially with strangers (Doyle et al., 2004; Gosch & Pankau, 1994). Alongside this increased social drive, the WS phenotype includes visuospatial deficits, intellectual impairments, increased attention to faces, increased risk of cardiovascular disease (supravalvular aortic stenosis), and distinctly "elfin" facial features, including a broad forehead, wide mouth, upturn nose, full cheeks and lips (Doyle et al., 2004; Järvinen-Pasley et al., 2008). WS is caused by a hemizygous genetic deletion in chromosomal region 7q11.23 affecting approximately 25-28 genes (Korenberg et al., 2000). The clinical diagnosis of WS is confirmed via fluorescent *in situ* hybridization (FISH) analysis, which may confirm a deletion within the WS chromosomal region (Williams Syndrome Association, 2019).

The social profile of WS is denoted by the predominant affiliative behavior with intellectual and visuospatial deficits (Bellugi et al. 2000), but also includes strengths in language ability, such as verbal short-term memory, working memory, and vocabulary (Mervis et al. 2003) and increased attention to faces (Järvinen-Pasley et al., 2008). WS individuals ranking of happy faces (Haas et al., 2009) and unfamiliar faces as more approachable (Bellugi, Adolphs, Cassady, & Chiles, 1999) with an inability to detect facial fear signals appropriately (Plesa-Skwerer et al. 2006; Plesa-Skwerer et al. 2011). Williams syndrome has several known targets of the body

caused by the genetic deletion. Mouse models of the WS deletion have demonstrated similar social and physiological phenotypes, such as more affiliative behavior and cardiovascular abnormalities (Osborne, 2010; Young et al., 2008). The deletion of the elastin-encoding gene *ELN* has been well-documented as a contributing factor to the high rate of cardiac disease, such as SVAS (narrowing of the aorta), which is the common cause of death in WS individuals (Pober, 2010; Wessel, Pankau, Kececioglu, Ruschewski, & Bürsch, 1994). The mechanisms underlying the somatic physical phenotype of WS is well-characterized; however, while genes in the WS deletion such as GTF2IRD1, CYCLN2, and LIMK1 have been implicated in social cognition, emotional behavior (particularly fear), and neuronal development (Arber et al., 1998; Donnai & Karmiloff-Smith, 2000; Porter et al., 2012; Serrano-Juárez et al., 2018; van Hagen et al., 2007; Young et al., 2008), little is known about the neuroanatomical correlates of the distinct hypersocial phenotype.

Williams syndrome poses a unique opportunity to study known genetic deletions that result in a characteristic, consistent social phenotype and many studies have been conducted in unraveling WS at the genetic and behavioral levels (Martens et al., 2008). What is rather lacking in research is the bridge between the two levels: the affected anatomy, particularly the brain microstructure. For example, the *ELN* gene is largely recognized as a major contributor to cardiac complications in WS individuals, epitomizing the genotype-phenotype relationship (Donnai & Karmiloff-Smith, 2000). However, the neurological underpinnings of the hypersocial phenotype is not well-understood and examining the microstructure of brain regions linked to sociobehavioral circuitry are critical in bridging the gap between genotype, neuroanatomy, and behavior.

The Amygdala

The amygdala is a social brain structure that converges on social behavior and emotion (Brothers, 1990). The amygdala is a subcortical structure located in the medial temporal lobe and is typically known as pivotal region for emotional information processing, especially fear (Davis, 1992; Ochsner & Gross, 2005). Additionally, this region serves as a central point for evaluating social and emotional information in the brain (Adolphs 2003; Klüver and Bucy 1939; Murray 2007). A well-documented case demonstrating the function of the amygdala involved Patient S.M. who was diagnosed with Urbach-Weithe disease, an autosomal recessive condition causing bilateral amygdala destruction (Adolphs et al. 1994). With virtually absent amygdala function, Patient S.M. shows a seemingly "fearless" behavior and could not experience fear when posed with typically fearful stimuli, particularly fearful facial expressions (Adolphs et al. 1994). While intellectual and memory capabilities as well as sensory association areas are conserved, Patient S.M. is unable to identify fearful situations that may be life-threatening (Feinstein et al., 2011; Kluver and Bucy, 1939). Subsequent human studies have shown the role of the amygdala in threat detection (Mattavelli et al., 2014), fear conditioning, and fear learning (Rodrigues, Schafe, & LeDoux, 2004). Lesion studies of the amygdala in macaques have demonstrated similar behaviors, such as abnormal threat detection, less social stress, more affiliative behavior (Emery et al., 2001) and lack of fear responses to unfamiliar objects (Amaral, 2002; Dal Monte, Costa, Noble, Murray, & Averbeck, 2015).

The amygdala is composed of 13 distinct nuclei, or subregions (Sah et al. 2003). Each defined by neuronal morphology, electrophysiology, function, and/or connectivity to other brain regions (Sah et al. 2003). The four nuclei in the amygdala commonly examined and distinguished in this study include the lateral, basal, accessory basal (together referred to as the

basolateral nucleus) and the central nucleus, because of their robust boundaries and specialized connectivity. Each nucleus has an important role in the bidirectional relay of sensory information to many cortical and subcortical regions, as well as integrating that information between the nuclei. The lateral nucleus is the primary input region for the connecting sensory information (gustatory, somatosensory, auditory, visual) from the cortical areas, thalamus, temporal lobe, and nucleus accumbens with bidirectional connections (Sah et al. 2003; Stefanacci & Amaral 2000). The basal nucleus receives information from the prefrontal, orbitofrontal, temporal cortices (perirhinal and parahippocampal) with projections from lateral nucleus (Stefanacci & Amaral, 2002; Stefanacci, Suzuki, & Amaral, 1996). The accessory basal nucleus receives similar information as the basal nucleus with additional input from insular cortex and lateral nucleus intrinsically (Stefanacci & Amaral, 2002). The central nucleus receives strong intrinsic amygdaloid nuclei information from the basolateral region and from the insular cortex but notably serves as the primary output region to autonomic and visceral structures in the brainstem (midbrain, pons, and medulla) (Price & Amaral 1981; Sah et al. 2003; Stefanacci & Amaral 2002). In a general sense, sensory information is mainly received within the basolateral nuclei complex and projected out of the amygdala by the central nucleus (LeDoux, 2007). The differentiated amygdala nuclei receive information from many sensory modalities and similarly project to many other brain regions making this structure integral to social, emotional, and cognitive circuits (Sah et al. 2003). Disruption to the amygdala may result in improper network communication and atypical phenotypes depending on the region information being transmitted throughout the amygdala (Prager et al., 2016). The amygdala is therefore of interest in WS because of its central role in socio-emotional information processing and could be a point of disruption resulting in an atypical social and emotional behavior.

Amygdaloid Neurons

The balance of excitatory and inhibitory neuron firing dictates the neuronal activity of neurons and, therefore, the overall amygdaloid nuclei activity. The main populations of amygdala neurons, mostly studied in the basolateral nuclei, are glutamatergic excitatory principal neurons, which comprise approximately 80-90% of total neurons, similar to the cortex (Markram et al., 2004; McDonald & Augustine, 1993; Pitkänen & Amaral, 1994). The remaining are mainly local GABAergic inhibitory interneurons that regulate glutamatergic excitatory principal neurons as well as other interneurons (McDonald & Augustine, 1993). By releasing GABA, an inhibitory neurotransmitter, in their synaptic connections to excitatory neurons, creates an inhibitory post-synaptic signal causing a local chemical environment to prevent firing activity of the post-synaptic neuron. This action allows for inhibitory interneurons to regulate and balance neurotransmission. GABAergic interneurons can be categorized by several parameters such as electrophysiology and morphology, but the most common method is by their protein markers in *post mortem* tissue. The primary inhibitory interneurons of the amygdala are those immunoreactive for the protein markers calbindin, calretinin, and parvalbumin, which can be solely or co-expressed in various combinations (McDonald & Mascagni, 2001; Spampanato et al., 2011).

Parvalbumin-positive (PV+) interneurons have been extensively studied and profiled as a major amygdala interneuron subtype. PV+ interneurons express the calcium-binding protein parvalbumin. Parvalbumin is primarily used as a neuronal marker in immunohistochemistry and is also present in fast-twitch muscle fibers in addition to neural tissue (Celio & Heizmann, 1982). In the rat amygdala, 19-43% of the total GABAergic interneuron population in the amygdala is PV+ (McDonald & Mascagni, 2001). In the macaque amygdala, PV+ interneurons represent

approximately 29-38% of the GABAergic interneuron population (Mascagni, Muly, Rainnie, & McDonald, 2009). There are has yet to be a human study denoting the percentage of PV+ interneuron within the GABAergic population, however, PV+ interneurons were measured as <1% of the total neuron population (Garcia-Amado & Prensa, 2010). Qualitatively, PV+ interneuron density is similar across rat, monkey, and human, with the highest density within the lateral nucleus and sparse in more medial nuclei (Pitkänen & Kemppainen 2002).

GABAergic PV+ interneurons function to control the excitability of single principal neurons and other interneurons, as well as synchronizing the frequency of groups of principal neurons (Cobb et al., 1995; Spampanato et al., 2011; Woodruff et al., 2006; Woodruff & Sah, 2007b). PV+ interneurons are distinct from other interneuron populations by their fast-spiking firing activity, both in burst and stuttering patterns (Rainnie et al., 2006; Woodruff & Sah, 2007b) and are also morphologically distinct, with chandelier and basket cell-like synapses (Muller, Mascagni, & McDonald, 2006; H. Sorvari et al., 1996). PV+ interneurons contact their targets at the soma, like a basket cell, and the axon initial segment where action potentials start, like a chandelier cell (McDonald and Betette 2001; Muller, Mascagni, and McDonald 2006; Woodruff and Sah 2007). PV+ interneurons are involved in feedforward and feedback inhibition and excitation systems dependent on the type of afferent cell, glutamatergic or interneuron respectively (Woodruff et al., 2006; Woodruff & Sah, 2007a, 2007b).

Consistent across primate, rat, and cat species, the distribution of PV+ interneurons varies across the amygdaloid nuclei, where the lateral nucleus contains the highest density and the basal, accessory basal, and central nuclei show a decreasing density with virtually none in the central nucleus (Pantazopoulos et al. 2006; Garcia-Amado and Presna 2010; Sorvari et al. 1995). Although, the central nucleus is densely populated with GABAergic interneurons in macaques

(McDonald & Augustine, 1993), PV+ interneurons are not the most prevalent population in this region for humans.

Due to PV+ interneurons' role in the direct regulation of excitatory activity within the amygdala, it is possible that PV+ interneuron number or density alteration can cause improper amygdala function. Given the amygdala's role in socio-emotional information processing, amygdala dysfunction may underly social behavior-linked disorders (Schumann, Bauman, and Amaral 2011), possibly due to irregularities in the interneuronal regulation system (Coghlan et al., 2012b; Marín, 2012).

Neurological Disorders: Interneuron System and the Amygdala

Both the inhibitory interneuron system and the amygdala have been implicated in several neurological disorders that include atypical mental and behavioral phenotypes, such as autism spectrum disorders (ASD), Fragile X syndrome (FXS), Rett syndrome, and schizophrenia (Berretta et al., 2007; Prager et al., 2016; Schumann et al., 2011). These two aspects, the interneuron system and the amygdala, will be described sequentially in the following neurological disorders.

Autism Spectrum Disorders

The sociobehavioral phenotype in WS has been described as being antithetical to ASD because it has been referred to as WS's opposite social phenotype, due to ASD's characteristically reserved social approach behavior and disinhibited hypersocial approach behavior observed in WS (Asada & Itakura, 2012; Barak & Feng, 2016; Vivanti, Hamner, & Lee, 2018). Additionally, there is a pattern of overlap seen in the 7th chromosome in select cases of ASD where the WS chromosomal region is duplicated in ASD (Sanders et al., 2011). An

overall decrease of GABAergic inhibitory activity in the amygdala has been observed, which may contribute to the typical ASD reserved social phenotype (Coghlan et al., 2012). Additionally, there is a significant decrease of PV+ interneurons across the cortex in ASD, notably within the prefrontal cortex, a region strongly connected with the amygdala (Hashemi, Ariza, Rogers, Noctor, & Martínez-Cerdeño, 2017; Selby, Zhang, & Sun, 2007). In an ASD mouse model, there is reduced PV+ interneuron GABA release in the cortex (Cellot & Cherubini, 2014). In autistic-like CADPS2-knockout mice, CADPS2 being a calcium mediator gene located on chromosome 7, there is a decrease of neocortical PV+ interneurons (Sadakata et al., 2007). If the implicated decrease of inhibitory regulation within a socio-emotional processing region is supported for ASD, then the opposite may be true for WS.

The ASD amygdala demonstrates cellular and structural changes compared to controls. Children with ASD have shown an increase in amygdala volume which is not continued into adolescence (Schumann et al. 2004). There is a significant decrease in total neuron number within the amygdala and lateral nucleus in ASD individuals (Schumann and Amaral 2006). These results interestingly contrast with the WS amygdala anatomical findings described later in this section.

Fragile X Syndrome

FXS is caused by the disruption to fragile X mental retardation 1 protein (FMR1) gene causing intellectual disabilities and causes autistic-like behaviors (Garber, Visootsak, & Warren, 2008). FXS has shown decreased inhibitory elements in the mouse amygdala including inhibitory neurotransmission, inhibitory synapses, synaptic GABA and GAD65/67 levels (Olmos-Serrano et al., 2010) and a reduction in the number of GABAergic receptors (Vislay et

al., 2013). Amygdala volume has demonstrated volumetric decreases in all ages in FXS (Gothelf et al. 2008; Schumann, Bauman, and Amaral 2011), FXS individuals have a decreased amygdala response in the presence of fearful faces (Kim et al., 2014). These studies collectively demonstrate that the amygdala may be a point of disruption in a genetically linked neurodevelopmental disorder.

Rett Syndrome

Rett syndrome is a neurodevelopmental disorder caused by genetic mutation in methyl-CpG-binding protein 2, MeCP2, controlling chromatin remodeling and RNA splicing, resulting loss of motor functions, reserved social behavior, and a range of mental retardation occurring predominantly in females (Chahrour & Zoghbi, 2007). In MeCP2-knockout mouse models, the MeCP2 deficiency results in decreased GABAergic inhibitory interneuron activity while exhibiting Rett syndrome like behaviors (Chao et al., 2010). There have been contrasting reports on the levels of GABA within Rett syndrome individuals, where there is an increase of GABA within the basal ganglia and frontal cortex in Rett syndrome girls which then significantly decrease with age (Blue, Naidu, & Johnston, 1999a, 1999b). Rett syndrome-like mouse models demonstrated 39% amygdala volume reduction, as well as reductions in related social-cognitive structures like the hippocampus and striatum (Stearns et al., 2007).

Schizophrenia

Schizophrenia is a psychiatric disorder exhibiting psychotic symptoms such as delusions and hallucinations, disorganized speech, and social withdrawal (Volk & Lewis, 2015) with proposed neurodevelopmental origins (Birnbaum and Weinberger 2017; Murray et al. 1992).

Schizophrenic mice demonstrated atypical PV+ interneuron activity within the amygdala (Marín, 2012). The prefrontal cortex is a highly connected brain region with the amygdala (Stefanacci & Amaral, 2000) and has demonstrated a reduction in the expression of GAD67, the precursor molecule for GABA (Akbarian et al., 1995), a reduction of GABAergic connections such as varicosities and axon terminals of PV+ cells in human schizophrenic subjects (Lewis et al., 2001; Woo, Whitehead, Melchitzky, & Lewis, 1998), and genetic candidates that contribute to PV+ interneuron development that include improper PV+ interneuron functioning have been found to be affected in schizophrenia-like mice (del Pino et al., 2013). The hippocampus is a brain structure that receives strong projections from the amygdala and has "partially" demonstrated that excess excitatory input from the amygdala pathway induce changes to the GABAergic system (GAD67+ terminal density) within the hippocampus (Berretta, Munno, & Benes, 2001).

Amygdala volume has been shown to be comparatively decreased in childhood and increased during adolescence, where amygdala studies seem to be dependent on subject age, severity of symptoms, and concurrent medications (Schumann, Bauman, and Amaral 2011). Lateral nucleus volume is also decreased in schizophrenic individuals (Kreczmanski et al., 2007).

Williams Syndrome

Above are examples of neurodevelopmental disorders that inhibitory interneuron modulation and/or amygdala structural differences, however little is known about WS amygdala structure *post mortem,* and no studies to date have examined inhibitory interneuron populations in the WS amygdala, only within preliminary studies within WS basal ganglia (Dr. Kari Hanson, personal communication).

Disruptions to brain anatomical structure and activity have been implicated in WS. MRI studies have shown some of the highly implicated brain regions in WS. There is a global reduction of brain volume in WS adults (Jernigan and Bellugi 1990; Reiss et al. 2000). Prior *post mortem* studies, in addition to the neuroimaging studies above, have been conducted investigating the WS amygdala structure and neuronal composition. Amygdala volume (Reiss et al. 2004) and basolateral neuron density are increased in WS compared to neurotypical individuals (Lew et al. 2018; Martens, Wilson, Dudgeon, & Reutens, 2009). At a functional level, normal amygdala activity is reduced compared to typically-developing controls in the presence negative social stimuli, such as threatening or fearful faces (Haas et al., 2009; Meyer-Lindenberg et al., 2005), epitomizing a dampened social fear response. Brain structures that share bidirectional connections to the amygdala, such as the prefrontal cortex and striatum, have been documented to have total neuron density difference in the WS brain compared to neurotypical controls (Lew et al., 2017).

The collection of these neuroanatomical studies demonstrate that Williams syndrome contains neuroanatomical changes that may be contributing to the characteristic hypersocial phenotype. Specifically, the GABAergic system within WS is an area of interest for this disorder because of the evident modulation in other neurodevelopmental disorders with atypical social behaviors. The GABAergic system within WS hasn't been extensively explored, in part due to the scarcity of *post mortem* materials.

Present Study

Given the critical role of the amygdala in social behavior, William syndrome's unique hypersocial drive, and the role of the inhibitory interneuron system in modulating behavioral

circuitry, the inhibitory regulation of the amygdala of WS is a potential site of dysfunction. This pilot study is the first to measure an important inhibitory interneuron population within the amygdala of Williams syndrome individuals. Utilizing immunohistochemical and unbiased stereological techniques, the PV+ interneuron density was measured within the four main nuclei of the amygdala in *post mortem* tissue of four WS and age-, sex-, and hemisphere-matched neurotypical control pairs. We will investigate whether the units of the inhibitory networks within the amygdala may be atypical within WS. I hypothesized that the seemingly uninhibited hypersocial WS phenotype may be the result of a higher PV+ inhibitory interneuron density with the amygdala, a highly innervated socio-emotional processing area of the brain, due to the greater inhibitory regulation neurons that would be present. With greater inhibitory interneuron presence, it is speculated that there would be greater inhibition of the fear/threat detection ability of the amygdala reflected in a "fearless" uninhibited social approach, such as the WS social phenotype. This investigation can lay a stepping stone for further quantitative neuroanatomical studies of Williams syndrome and other neurodevelopmental disorders with distinct social phenotypes looking into the GABAergic system and the amygdala.

CHAPTER 3: CONCLUSIONS

The multidisciplinary nature of this study integrates unique biological techniques, utilizes human *post mortem* tissue, pinpoints a minor population of neurons, and profiles a rare neurodevelopmental disorder. As a result of the combination of these factors, this pilot study is the first of its kind to quantitatively measure the inhibitory interneuron system within amygdala in Williams syndrome and one of few with human subjects.

Histological and stereological techniques are fundamental methods of research allowing for the hands-on analysis of affected tissue and anatomy. *Post mortem* histology, especially, is a rare opportunity in biological research because of the limited amount of tissue donated, even more so within the realm of rare neurodevelopmental disorders. The infrequency of WS and subsequent infrequent *post mortem* WS brain tissue is an incredibly rare opportunity for scientists. Projects using this tissue must be carefully considered and strategic because of the limited number of tissue sections, resulting in few but novel studies. I have been privileged to be able to access this rare material and contribute to the neuroanatomical aspects of WS.

Another aspect of this study that measures the inhibitory interneurons which constitute a small fraction of total neurons both within the amygdala and the greater cortex. Interneurons, although low in presence, are a pivotal source of circuit regulation in neuronal networks. This measure of density requires a threshold number of cells to quantify in order for reliable error analysis and therefore reasonable conclusions to be made. This study was no exception to this pitfall, however, contributes to infrequent human studies exploring inhibitory neurocircuitry.

The convergence of each unique aspect in the present study made these findings not only novel, but a stepping stone for future studies to continue to unravel the unique genotype-phenotype relationship WS embodies. From here, future studies in WS may pursue interneuron

density measurements in other social, emotional, and or cognitive brain regions to observe GABAergic system disruptions, such as the hippocampus, prefrontal cortex, and orbitofrontal cortex. Within the amygdala, more inhibitory interneuron subpopulations as well as the entire GABAergic system could be quantified to create a more complete amygdala GABAergic system story. This PV+ interneuron density measurement technique can also be applied to related neurological/neurodevelopmental disorders to measure the GABAergic composition and relate the findings across conditions that have overlapping developmental origins or implicated genes, such as ASD, Fragile X syndrome, schizophrenia, and anxiety disorders. Additionally, PV+ interneuron density can be measured in animal models to not only retrieve the corresponding *post mortem* anatomical correlates in other species, but complementary functional activity.

Overall this study serves as one of the first studies to implicate the GABAergic system in WS, although with no significant differences in the WS phenotype. This study contributes to the neuroanatomical underpinnings of the disorder, however further pursuit of the inhibitory interneuron measurement within this structure as well as other brain structures may reveal differences that can serve as potential therapeutic targets to treat the accompanying, potentially harmful, symptoms of WS.

APPENDIX

Table 1. Age-, sex-, and brain hemisphere-matched subjects included in this study. PMI is abbreviated for *post mortem* interval.

Subject	Condition	Age at death (years)	Sex	Hemisphere	PMI (hours)	Cause of death
WS10	WS	17	Male	Right	24	Cardiac complications
NT4916	Control	19	Male	Right	5	Drowning
WS14	WS	42	Female	Right	18	Cardiac complications
NT5445	Control	42	Female	Right	10	Pulmonary thromboembolism
WS9	WS	43	Female	Right	12	Cardiac complications
NT5758	Control	43	Female	Right	22	Sepsis
WS13	WS	69	Male	Right	8	Cardiac complications
NT5943	Control	69	Male	Right	23	Acute coronary artery thrombosis

Table 2. Density measures for all Williams syndrome and neurotypical subject pairs. Each WS individual's matched subject pair is listed immediately below. CE represent coefficient of error. % total density represents percentage of PV+ interneuron density of total neuron density. * = values require additional quantification for calculation.

Subject	Amygdaloid Nucleus	Total neuron count	Estimated total population (neurons)	CE	Volume (mm^3)	Density ($neurons/mm^3$)	% total density
WS10							
	Lateral	285	44908.53	0.06	435.144	**103.204**	1.031
	Basal	52	5949.33	0.14	195.443	**30.440**	0.298
	Accessory Basal	57	3000.40	0.14	95.362	**31.463**	0.270
	Central	31	661.27	0.18	13.557	**48.779**	0.467
NT4916							
	Lateral	208	29227.46	0.08	387.130	**75.498**	0.633
	Basal	110	14211.84	0.11	292.787	**48.540**	0.294
	Accessory Basal	30	1620.89	0.18	145.765	**11.120**	0.082
	Central	1	37.12	1.00	9.949	**3.731**	0.023
WS14							
	Lateral	518	77961.87	0.05	454.527	**171.523**	1.374
	Basal	109	15277.55	0.11	246.218	**62.049**	0.492
	Accessory Basal	78	4701.18	0.13	136.714	**34.387**	0.276
	Central	14	441.17	0.27	21.251	**20.760**	0.155
NT5445							
	Lateral	336	57930.00	0.06	360.097	**160.873**	1.485
	Basal	62	6711.69	0.13	232.667	**28.847**	0.254
	Accessory Basal	5	363.29	0.45	105.208	**3.453**	0.027
	Central	1	0	1.00	23.921	**0**	0.000
WS9							
	Lateral	307	47274.93	0.06	445.676	**106.075**	0.842
	Basal	66	7497.44	0.13	199.022	**37.6714**	0.230
	Accessory Basal	31	1488.36	0.18	133.447	**11.153**	0.112
	Central	0	0	1.00	13.6146	**0**	0.000
NT5758							
	Lateral	41	6287.78	0.16	454.057	**13.848**	0.139
	Basal	158	13297.41	0.11	280.831	**47.3502**	0.435
	Accessory Basal	604	22865.27	0.06	85.7065	**266.786**	1.928
	Central	91	1704.01	0.12	9.688	**175.888**	1.572
WS13							
	Lateral	281	35103.79	0.06	315.548	**111.247**	*
	Basal	41	3970.30	0.16	202.149	**19.641**	*
	Accessory Basal	21	859.83	0.22	81.158	**10.595**	*
	Central	4	74.54	0.50	20.439	**3.647**	*
NT5943							
	Lateral	289	44209.00	0.08	320.108	**138.109**	*

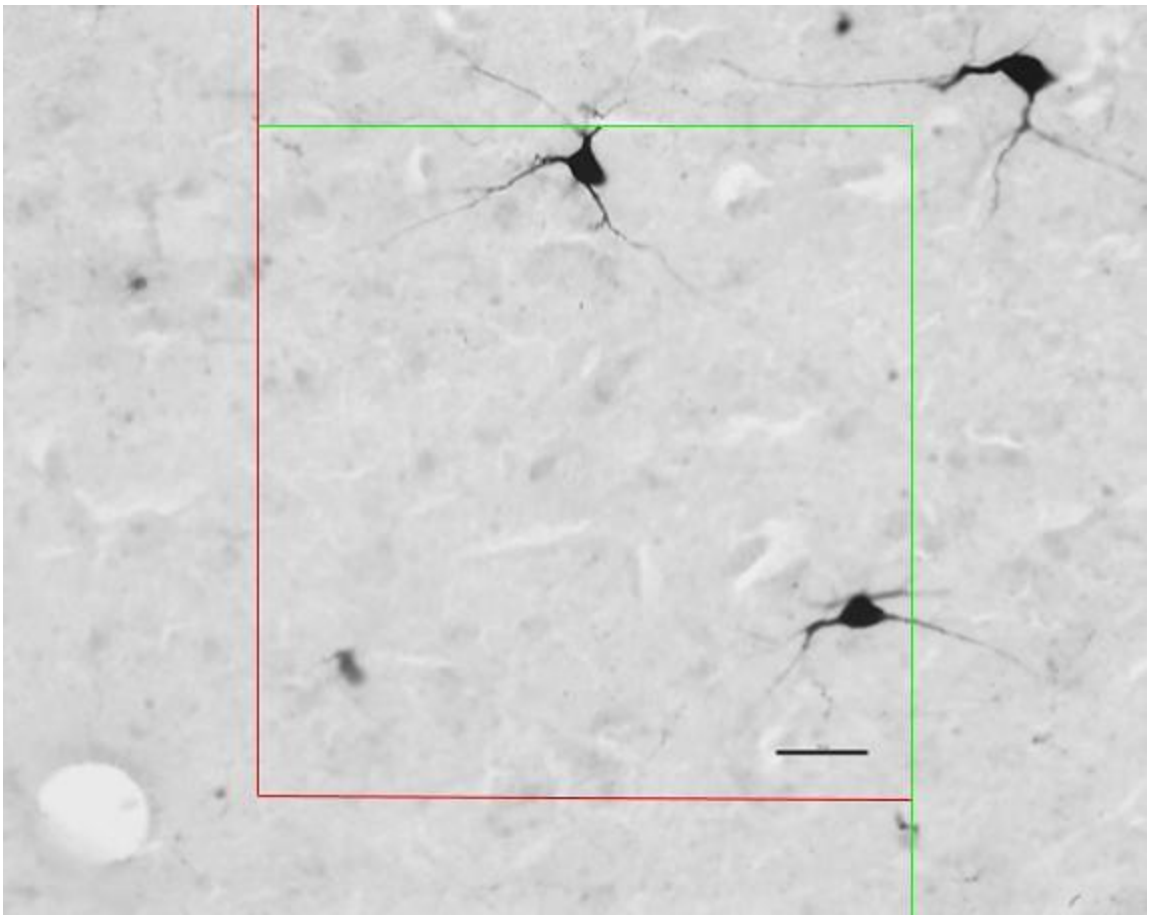

Figure 1. Brightfield photomicrograph of PV+ immunostained amygdala tissue section in the Stereoinvestigator Optical Fractionator probe (20x magnification). PV+ interneurons (darkly stained cells) were counted when they appeared the counting frame, or intersected the green inclusion line, but not when they intersected the red exclusion line. Scale bar = 50 microns.

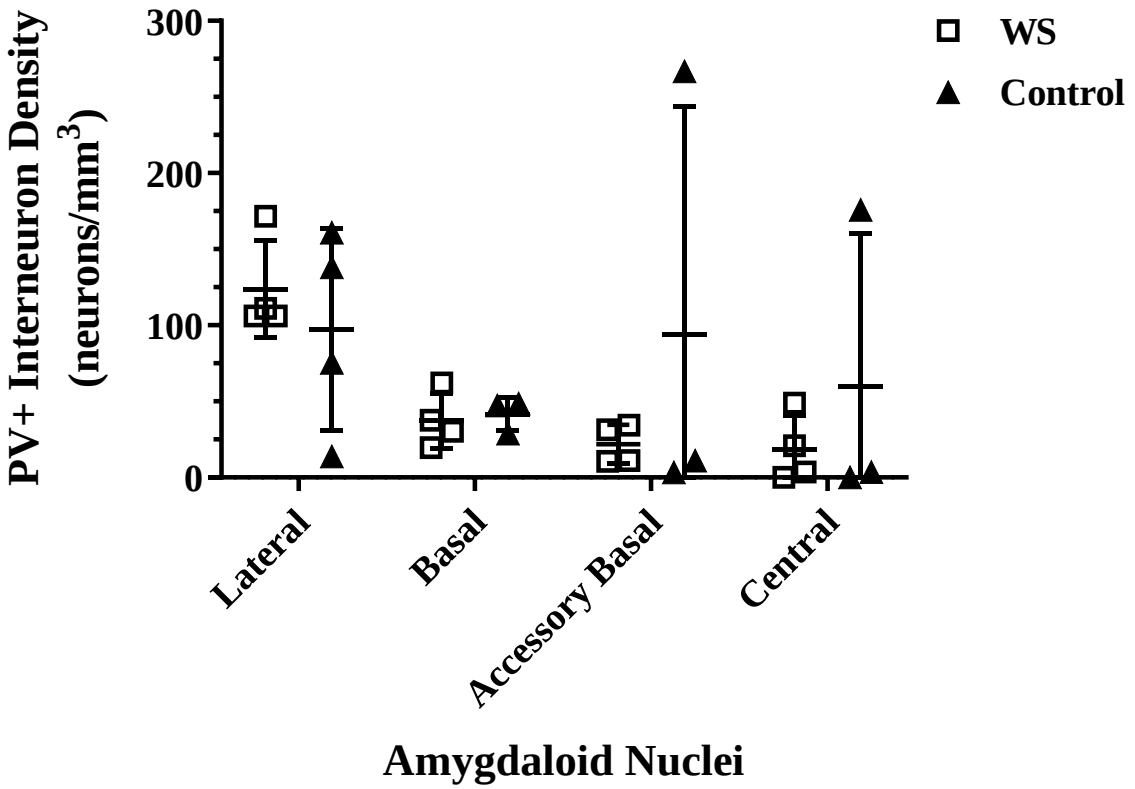

Figure 2. Parvalbumin-positive (PV+) interneuron density of *post mortem* human amygdala in Williams syndrome (WS) compared to neurotypical (NT) controls across four characterized amygdaloid nuclei. Individual values (each marker) and group means with standard deviations are included.

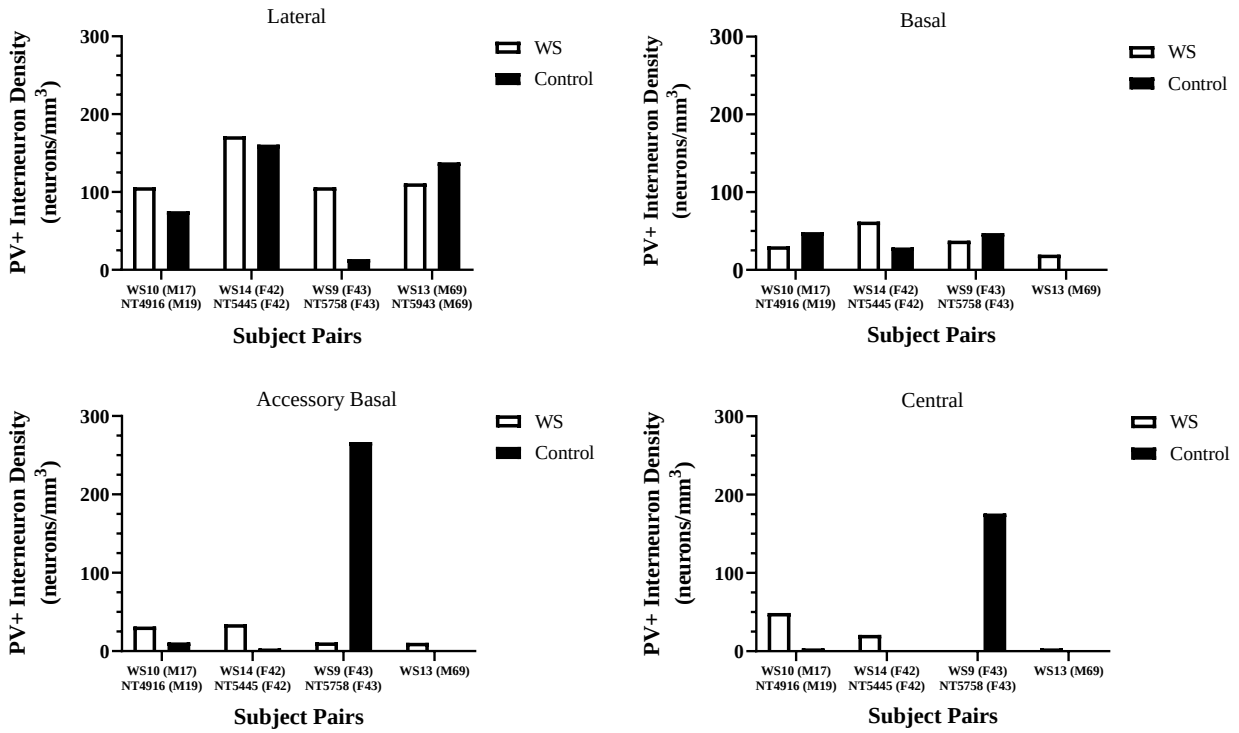

Figure 3. Individual values of parvalbumin-positive (PV+) interneuron density of *post mortem* human amygdala comparing Williams syndrome and neurotypical control groups per amygdaloid nuclei, each graph separates each nuclei. Subjects are labelled by condition then subject ID, followed by sex and age. For example, WS10 (M17) represents Williams syndrome subject 10, male, and 17 years old.

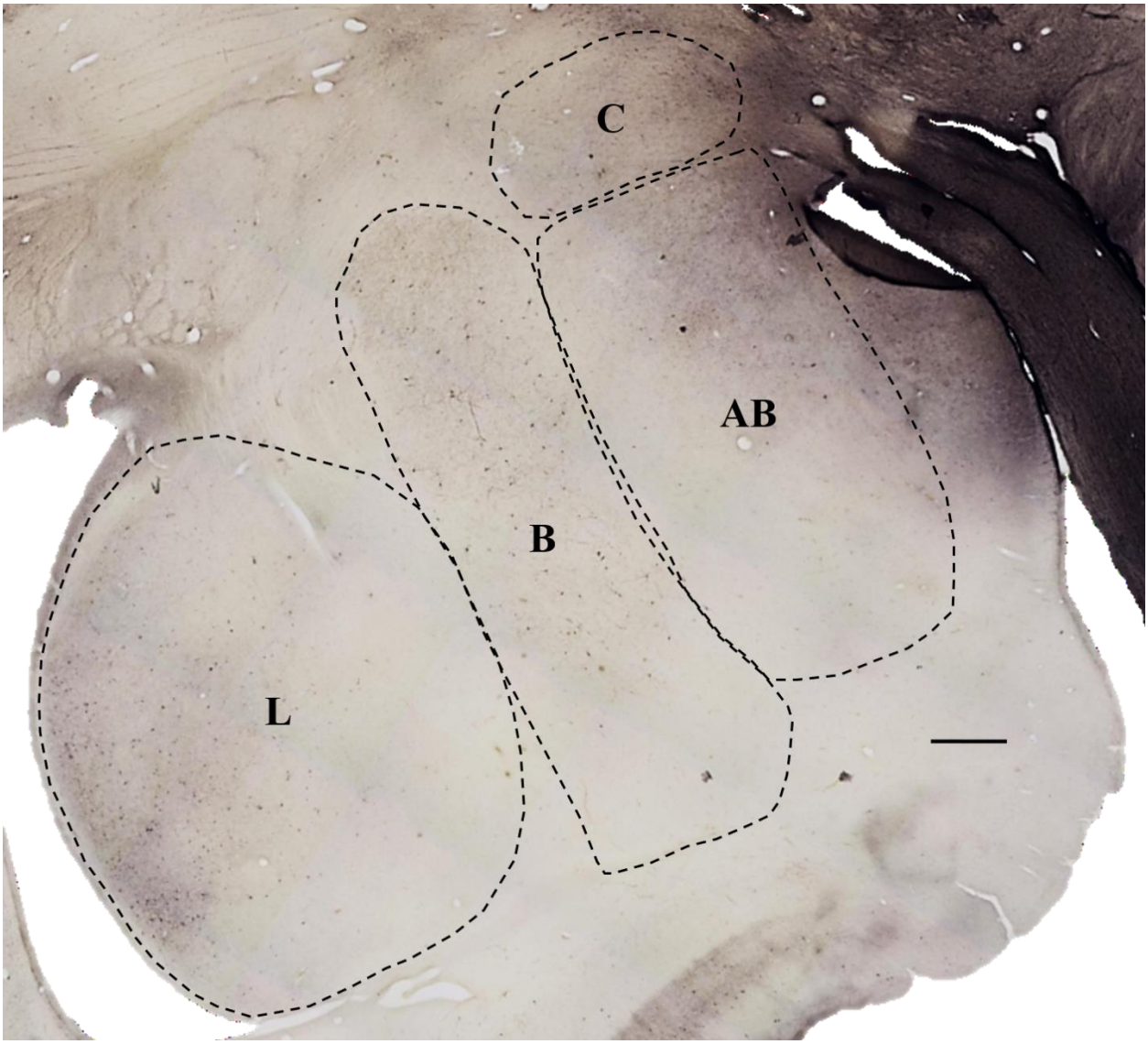

Figure 4. Brightfield photomicrograph of parvalbumin immunostained mid-amygdala tissue with major nuclei subdivision boundaries outlined in the coronal plane (WS14). Lateral (L), basal (B), accessory basal (AB), and central (C) nuclei are denoted in their respective boundary outlines. Photomicrograph captured and boundaries drawn at 1x magnification. Scale bar = 1 millimeter.

REFERENCES

Adolphs, R., Tranel, D., Damasio, H., & Damasio, A. (1994). Impaired recognition of emotion in facial expressions following bilateral damage to the human amygdala. *Nature*, *372*(6507), 669–672. https://doi.org/10.1038/372669a0

Adolphs, R. (2003). Is the human amygdala specialized for processing social information? *Annals of the New York Academy of Sciences*, *985*, 326–340. Retrieved from http://www.ncbi.nlm.nih.gov/pubmed/12724168

Akbarian, S., Kim, J. J., Potkin, S. G., Hagman, J. O., Tafazzoli, A., Bunney, W. E., & Jones, E. G. (1995). Gene expression for glutamic acid decarboxylase is reduced without loss of neurons in prefrontal cortex of schizophrenics. *Archives of General Psychiatry*, *52*(4), 258–266. Retrieved from http://www.ncbi.nlm.nih.gov/pubmed/7702443

Amaral, D. G. (2002). The primate amygdala and the neurobiology of social behavior: implications for understanding social anxiety. *Biological Psychiatry*, *51*(1), 11–17. https://doi.org/10.1016/S0006-3223(01)01307-5

Amaral, D. G., Schumann, C. M., & Nordahl, C. W. (2008). Neuroanatomy of autism. *Trends in Neurosciences*, *31*(3), 137–145. https://doi.org/10.1016/J.TINS.2007.12.005

Arber, S., Barbayannis, F. A., Hanser, H., Schneider, C., Stanyon, C. A., Bernard, O., & Caroni, P. (1998). Regulation of actin dynamics through phosphorylation of cofilin by LIM-kinase. *Nature*, *393*(6687), 805–809. https://doi.org/10.1038/31729

Asada, K., & Itakura, S. (2012). Social phenotypes of autism spectrum disorders and Williams syndrome: similarities and differences. *Frontiers in Psychology*, *3*, 247. https://doi.org/10.3389/fpsyg.2012.00247

Barak, B., & Feng, G. (2016). Neurobiology of social behavior abnormalities in autism and Williams syndrome. *Nature Neuroscience*. https://doi.org/10.1038/nn.4276

Belforte, J. E., Zsiros, V., Sklar, E. R., Jiang, Z., Yu, G., Li, Y., Quinlan, E. M., Nakazawa, K. (2010). Postnatal NMDA receptor ablation in corticolimbic interneurons confers schizophrenia-like phenotypes. *Nature Neuroscience*, *13*(1), 76–83. https://doi.org/10.1038/nn.2447

Bellugi, U., Adolphs, R., Cassady, C., & Chiles, M. (1999). Towards the neural basis for hypersociability in a genetic syndrome. *Neuroreport*, *10*(8), 1653–1657. Retrieved from http://www.ncbi.nlm.nih.gov/pubmed/10501552

Berretta, S., Munno, D. W., & Benes, F. M. (2001). Amygdalar activation alters the hippocampal GABA system: ?Partial? modelling for postmortem changes in schizophrenia. *The Journal of Comparative Neurology*, *431*(2), 129–138. https://doi.org/10.1002/1096-9861(20010305)431:2<129::AID-CNE1060>3.0.CO;2-6

Berretta, S., Pantazopoulos, H., & Lange, N. (2007). Neuron Numbers and Volume of the

Amygdala in Subjects Diagnosed with Bipolar Disorder or Schizophrenia. *Biological Psychiatry*, *62*(8), 884–893. https://doi.org/10.1016/J.BIOPSYCH.2007.04.023

Birnbaum, R., & Weinberger, D. R. (2017). Genetic insights into the neurodevelopmental origins of schizophrenia. *Nature Reviews Neuroscience*, *18*(12), 727–740. https://doi.org/10.1038/nrn.2017.125

Blue, M. E., Naidu, S., & Johnston, M. V. (1999a). Altered Development of Glutamate and GABA Receptors in the Basal Ganglia of Girls with Rett Syndrome. *Experimental Neurology*, *156*(2), 345–352. https://doi.org/10.1006/EXNR.1999.7030

Blue, M. E., Naidu, S., & Johnston, M. V. (1999b). Development of amino acid receptors in frontal cortex from girls with Rett syndrome. *Annals of Neurology*, *45*(4), 541–545. https://doi.org/10.1002/1531-8249(199904)45:4<541::AID-ANA21>3.0.CO;2-2

Celio, M. R., & Heizmann, C. W. (1982). Calcium-binding protein parvalbumin is associated with fast contracting muscle fibres. *Nature*, *297*(5866), 504–506. https://doi.org/10.1038/297504a0

Cellot, G., & Cherubini, E. (2014). GABAergic signaling as therapeutic target for autism spectrum disorders. *Frontiers in Pediatrics*, *2*, 70. https://doi.org/10.3389/fped.2014.00070

Chahrour, M., & Zoghbi, H. Y. (2007). The Story of Rett Syndrome: From Clinic to Neurobiology. *Neuron*, *56*(3), 422–437. https://doi.org/10.1016/J.NEURON.2007.10.001

Chao, H.-T., Chen, H., Samaco, R. C., Xue, M., Chahrour, M., Yoo, J., Neul, J. L., Gong, S., Lu, H.-C., Heintz, N., Ekker, M., Rubenstein, J. L., Noebels, J. L., Rosenmund, C., & Zoghbi, H. Y. (2010). Dysfunction in GABA signalling mediates autism-like stereotypies and Rett syndrome phenotypes. *Nature*, *468*(7321), 263–269. https://doi.org/10.1038/nature09582

Cobb, S. R., Buhl, E. H., Halasy, K., Paulsen, O., & Somogyi, P. (1995). Synchronization of neuronal activity in hippocampus by individual GABAergic interneurons. *Nature*, *378*(6552), 75–78. https://doi.org/10.1038/378075a0

Coghlan, S., Horder, J., Inkster, B., Mendez, M. A., Murphy, D. G., & Nutt, D. J. (2012a). GABA system dysfunction in autism and related disorders: from synapse to symptoms. *Neuroscience and Biobehavioral Reviews*, *36*(9), 2044–2055. https://doi.org/10.1016/j.neubiorev.2012.07.005

Dal Monte, O., Costa, V. D., Noble, P. L., Murray, E. A., & Averbeck, B. B. (2015). Amygdala lesions in rhesus macaques decrease attention to threat. *Nature Communications*, *6*(1), 10161. https://doi.org/10.1038/ncomms10161

Davis, M. (1992). The Role of the Amygdala in Fear and Anxiety. *Annual Review of Neuroscience*, *15*(1), 353–375. https://doi.org/10.1146/annurev.ne.15.030192.002033

DeFelipe, J. (2002). Chapter 17 Cortical interneurons: from Cajal to 2001. *Progress in Brain Research*, *136*, 215–238. https://doi.org/10.1016/S0079-6123(02)36019-9

del Pino, I., García-Frigola, C., Dehorter, N., Brotons-Mas, J. R., Alvarez-Salvado, E., Martínez de Lagrán, M., Ciceri, G., Gabaldón, M.V., Moratal, D., Dierssen, M., Canals, S., Marín, O., & Rico, B. (2013). Erbb4 Deletion from Fast-Spiking Interneurons Causes Schizophrenia-like Phenotypes. *Neuron*, *79*(6), 1152–1168. https://doi.org/10.1016/J.NEURON.2013.07.010

Donnai, D., & Karmiloff-Smith, A. (2000). Williams syndrome: from genotype through to the cognitive phenotype. *American Journal of Medical Genetics*, *97*(2), 164–171. Retrieved from http://www.ncbi.nlm.nih.gov/pubmed/11180224

Doyle, T. F., Bellugi, U., Korenberg, J. R., & Graham, J. (2004). ?Everybody in the world is my friend? hypersociability in young children with Williams syndrome. *American Journal of Medical Genetics*, *124A*(3), 263–273. https://doi.org/10.1002/ajmg.a.20416

Emery, N. J., Capitanio, J. P., Mason, W. A., Machado, C. J., Mendoza, S. P., & Amaral D. G. (2001). The effects of bilateral lesions of the amygdala on dyadic social interactions in rhesus monkeys (Macaca mulatta). *Behavioral Neuroscience*, *115*(3), 515-44. http://dx.doi.org/10.1037/0735-7044.115.3.515

Garber, K. B., Visootsak, J., & Warren, S. T. (2008). Fragile X syndrome. *European Journal of Human Genetics*, *16*(6), 666–672. https://doi.org/10.1038/ejhg.2008.61

Garcia-Amado, M., & Prensa, L. (2010). A quantitative study of the percentage of parvalbumin-positive interneurons and the dopaminergic fiber length density in the nuclear subdivisions of the human basolateral amygdaloid complex. In: Planner NM. 40th Annual Meeting of the Society for Neuroscience; November; San Diego, California, EEUU 2010. p. Program 909.24/LLL29

Gosch, A., & Pankau, R. (1994). Social-emotional and behavioral adjustment in children with Williams-Beuren syndrome. *American Journal of Medical Genetics*, *53*(4), 335–339. https://doi.org/10.1002/ajmg.1320530406

Gothelf, D., Furfaro, J. A., Hoeft, F., Eckert, M. A., Hall, S. S., O'Hara, R., Erba, H. W., Ringel, J., Hayashi, K. M., Patnaik, S., Golianu, B., Kraemer, H. C., Thompson, P. M., Piven, J., & Reiss, A. L. (2008). Neuroanatomy of fragile X syndrome is associated with aberrant behavior and the fragile X mental retardation protein (FMRP). *Annals of Neurology*, *63*(1), 40–51. https://doi.org/10.1002/ana.21243

Guidotti, A., Auta, J., Davis, J. M., Di-Giorgi-Gerevini, V., Dwivedi, Y., Grayson, D. R., Impagnatiello, F., Pandey, G., Pesold, C., Sharma, R., Uzunov, D., & Costa, E. (2000). Decrease in reelin and glutamic acid decarboxylase67 (GAD67) expression in schizophrenia and bipolar disorder: a postmortem brain study. *Archives of General Psychiatry*, *57*(11), 1061–1069. Retrieved from http://www.ncbi.nlm.nih.gov/pubmed/11074872

Haas, B. W., Mills, D., Yam, A., Hoeft, F., Bellugi, U., & Reiss, A. (2009). Genetic influences on sociability: heightened amygdala reactivity and event-related responses to positive social stimuli in Williams syndrome. *The Journal of Neuroscience : The Official Journal of the Society for Neuroscience*, *29*(4), 1132–1139. https://doi.org/10.1523/JNEUROSCI.5324-

08.2009

Hashemi, E., Ariza, J., Rogers, H., Noctor, S. C., & Martínez-Cerdeño, V. (2017). The Number of Parvalbumin-Expressing Interneurons Is Decreased in the Prefrontal Cortex in Autism. *Cerebral Cortex (New York, N.Y. : 1991)*, *27*(3), 1931–1943. https://doi.org/10.1093/cercor/bhw021

Järvinen-Pasley, A., Bellugi, U., Reilly, J., Mills, D. L., Galaburda, A., Reiss, A. L., & Korenberg, J. R. (2008). Defining the social phenotype in Williams syndrome: a model for linking gene, the brain, and behavior. *Development and Psychopathology*, *20*(1), 1–35. https://doi.org/10.1017/S0954579408000011

Jernigan, T. L., & Bellugi, U. (1990). Anomalous Brain Morphology on Magnetic Resonance Images in Williams Syndrome and Down Syndrome. *Archives of Neurology*, *47*(5), 529–533. https://doi.org/10.1001/archneur.1990.00530050049011

Ji, M.-H., Qiu, L.-L., Tang, H., Ju, L.-S., Sun, X.-R., Zhang, H., Jia, M., Zuo, Z.-Y., Shen, J.-C., & Yang, J.-J. (2015). Sepsis-induced selective parvalbumin interneuron phenotype loss and cognitive impairments may be mediated by NADPH oxidase 2 activation in mice. *Journal of Neuroinflammation*, *12*(1), 182. https://doi.org/10.1186/s12974-015-0401-x

Kataoka, Y., Kalanithi, P. S. A., Grantz, H., Schwartz, M. L., Saper, C., Leckman, J. F., & Vaccarino, F. M. (2010). Decreased number of parvalbumin and cholinergic interneurons in the striatum of individuals with Tourette syndrome. *The Journal of Comparative Neurology*, *518*(3), 277–291. https://doi.org/10.1002/cne.22206

Kemppainen, S., & Pitkanen, A. (2000). Distribution of parvalbumin, calretinin, and calbindin-D28k immunoreactivity in the rat amygdaloid complex and colocalization with ?-aminobutyric acid. *The Journal of Comparative Neurology*, *426*(3), 441–467. https://doi.org/10.1002/1096-9861(20001023)426:3<441::AID-CNE8>3.0.CO;2-7

Kim, S.-Y., Burris, J., Bassal, F., Koldewyn, K., Chattarji, S., Tassone, F., Hessl, D., & Rivera, S. M. (2014). Fear-specific amygdala function in children and adolescents on the fragile x spectrum: a dosage response of the FMR1 gene. *Cerebral Cortex (New York, N.Y. : 1991)*, *24*(3), 600–613. https://doi.org/10.1093/cercor/bhs341

Klüver, H., & Bucy, P. C. (1939). Preliminary analysis of functions of the temporal lobes in monkeys. *Archives of Neurology And Psychiatry*, *42*(6), 979. https://doi.org/10.1001/archneurpsyc.1939.02270240017001

Kordower, J. H., Piecinski, P., & Rakic, P. (1992). Neurogenesis of the amygdaloid nuclear complex in the Rhesus monkey. *Developmental Brain Research*, *68*(1), 9-15. https://doi.org/10.1016/0165-3806(92)90242-O

Korenberg, J. R., Chen, X. N., Hirota, H., Lai, Z., Bellugi, U., Burian, D., Roe, B., & Matsuoka, R. (2000). VI. Genome structure and cognitive map of Williams syndrome. *Journal of Cognitive Neuroscience*, *12 Suppl 1*, 89–107. Retrieved from http://www.ncbi.nlm.nih.gov/pubmed/10953236

Kreczmanski, P., Heinsen, H., Mantua, V., Woltersdorf, F., Masson, T., Ulfig, N., Schmidt-Kastner, R., Korr, H., Steinbusch, H. W., Hof, P. R., & Schmitz, C. (2007). Volume, neuron density and total neuron number in five subcortical regions in schizophrenia. *Brain*, *130*(3), 678–692. https://doi.org/10.1093/brain/awl386

LeDoux, J. (2007). The amygdala. *Current Biology : CB*, *17*(20), R868-74. https://doi.org/10.1016/j.cub.2007.08.005

Lever, A., & Mackenzie, I. (2007). Sepsis: definition, epidemiology, and diagnosis. *BMJ (Clinical Research Ed.)*, *335*(7625), 879–883. https://doi.org/10.1136/bmj.39346.495880.AE

Lew, C. H., Groeniger, K. M., Bellugi, U., Stefanacci, L., Schumann, C. M., & Semendeferi, K. (2018). A postmortem stereological study of the amygdala in Williams syndrome. *Brain Structure and Function*. https://doi.org/10.1007/s00429-017-1592-y

Lew, C. H., Brown, C., Bellugi, U., & Semendeferi, K. (2017). Neuron density is decreased in the prefrontal cortex in Williams syndrome. *Autism Research*, *10*(1), 99–112. https://doi.org/10.1002/aur.1677

Lewis, D. A., Cruz, D. A., Melchitzky, D. S., & Pierri, J. N. (2001). Lamina-Specific Deficits in Parvalbumin-Immunoreactive Varicosities in the Prefrontal Cortex of Subjects With Schizophrenia: Evidence for Fewer Projections From the Thalamus. *American Journal of Psychiatry*, *158*(9), 1411–1422. https://doi.org/10.1176/appi.ajp.158.9.1411

Marín, O. (2012). Interneuron dysfunction in psychiatric disorders. *Nature Reviews Neuroscience*, *13*(2), 107-120. https://doi.org/10.1038/nrn3155

Markram, H., Toledo-Rodriguez, M., Wang, Y., Gupta, A., Silberberg, G., & Wu, C. (2004). Interneurons of the neocortical inhibitory system. *Nature Reviews Neuroscience*, *5*(10), 793–807. https://doi.org/10.1038/nrn1519

Martens, M. A., Wilson, S. J., Dudgeon, P., & Reutens, D. C. (2009). Approachability and the amygdala: Insights from Williams syndrome. *Neuropsychologia*, *47*(12), 2446–2453. https://doi.org/10.1016/J.NEUROPSYCHOLOGIA.2009.04.017

Martens, M. A., Wilson, S. J., & Reutens, D. C. (2008). Research Review: Williams syndrome: a critical review of the cognitive, behavioral, and neuroanatomical phenotype. *Journal of Child Psychology and Psychiatry*, *49*(6), 576–608. https://doi.org/10.1111/j.1469-7610.2008.01887.x

Mascagni, F., Muly, E. C., Rainnie, D. G., & McDonald, A. J. (2009). Immunohistochemical characterization of parvalbumin-containing interneurons in the monkey basolateral amygdala. *Neuroscience*, *158*(4), 1541–1550. https://doi.org/10.1016/j.neuroscience.2008.11.017

Mattavelli, G., Sormaz, M., Flack, T., Asghar, A. U. R., Fan, S., Frey, J., Manssuer, L., Usten, D., Young, A. W., & Andrews, T. J. (2014). Neural responses to facial expressions support

the role of the amygdala in processing threat. *Social Cognitive and Affective Neuroscience*, *9*(11), 1684–1689. https://doi.org/10.1093/scan/nst162

McDonald, A., & Mascagni, F. (2001). Colocalization of calcium-binding proteins and GABA in neurons of the rat basolateral amygdala. *Neuroscience*, *105*(3), 681–693. https://doi.org/10.1016/S0306-4522(01)00214-7

McDonald, A. J., & Augustine, J. R. (1993). Localization of GABA-like immunoreactivity in the monkey amygdala. *Neuroscience*, *52*(2), 281–294. https://doi.org/10.1016/0306-4522(93)90156-A

McDonald, A. J., & Betette, R. L. (2001). Parvalbumin-containing neurons in the rat basolateral amygdala: morphology and co-localization of Calbindin-D28k. *Neuroscience*, *102*(2), 413–425. https://doi.org/10.1016/S0306-4522(00)00481-4

Meyer-Lindenberg, A., Hariri, A. R., Munoz, K. E., Mervis, C. B., Mattay, V. S., Morris, C. A., & Berman, K. F. (2005). Neural correlates of genetically abnormal social cognition in Williams syndrome. *Nature Neuroscience*. https://doi.org/10.1038/nn1494

Mikkonen, M., Soininen, H., & Pitkänen, A. (1997). Distribution of parvalbumin-, calretinin-, and calbindin-D28k-immunoreactive neurons and fibers in the human entorhinal cortex. *The Journal of Comparative Neurology*, *388*(1), 64–88. https://doi.org/10.1002/(SICI)1096-9861(19971110)388:1<64::AID-CNE5>3.0.CO;2-M

Morris, C. A., Demsey, S. A., Leonard, C. O., Dilts, C., & Blackburn, B. L. (1988). Natural history of Williams syndrome: Physical characteristics. *The Journal of Pediatrics*, *113*(2), 318–326. https://doi.org/10.1016/S0022-3476(88)80272-5

Muller, J. F., Mascagni, F., & McDonald, A. J. (2006). Pyramidal cells of the rat basolateral amygdala: synaptology and innervation by parvalbumin-immunoreactive interneurons. *The Journal of Comparative Neurology*, *494*(4), 635–650. https://doi.org/10.1002/cne.20832

Murray, E. A. (2007). The amygdala, reward and emotion. *Trends in Cognitive Sciences*, *11*(11), 489–497. https://doi.org/10.1016/J.TICS.2007.08.013

Murray, R. M., O'Callaghan, E., Castle, D. J., & Lewis, S. W. (1992). A Neurodevelopmental Approach to the Classification of Schizophrenia. *Schizophrenia Bulletin*, *18*(2), 319–332. https://doi.org/10.1093/schbul/18.2.319

Ochsner, K. N., & Gross, J. J. (2005). The cognitive control of emotion. *Trends in Cognitive Sciences*, *9*(5), 242–249. https://doi.org/10.1016/J.TICS.2005.03.010

Olmos-Serrano, J. L., Paluszkiewicz, S. M., Martin, B. S., Kaufmann, W. E., Corbin, J. G., & Huntsman, M. M. (2010). Defective GABAergic neurotransmission and pharmacological rescue of neuronal hyperexcitability in the amygdala in a mouse model of fragile X syndrome. *The Journal of Neuroscience : The Official Journal of the Society for Neuroscience*, *30*(29), 9929–9938. https://doi.org/10.1523/JNEUROSCI.1714-10.2010

Osborne, L. R. (2010). Animal models of Williams syndrome. *American Journal of Medical Genetics. Part C, Seminars in Medical Genetics*, *154C*(2), 209–219. https://doi.org/10.1002/ajmg.c.30257

Pantazopoulos, H., Lange, N., Hassinger, L., & Berretta, S. (2006). Subpopulations of neurons expressing parvalbumin in the human amygdala. *The Journal of Comparative Neurology*, *496*(5), 706–722. https://doi.org/10.1002/cne.20961

Pitkänen, A, & Amaral, D. G. (1994). The distribution of GABAergic cells, fibers, and terminals in the monkey amygdaloid complex: an immunohistochemical and in situ hybridization study. *The Journal of Neuroscience : The Official Journal of the Society for Neuroscience*, *14*(4), 2200–2224. https://doi.org/10.1523/JNEUROSCI.14-04-02200.1994

Pitkänen, A., & Amaral, D. G. (1993). Distribution of parvalbumin-immunoreactive cells and fibers in the monkey temporal lobe: The amygdaloid complex. *Journal of Comparative Neurology*, *331*(1), 14–36. https://doi.org/10.1002/cne.903310103

Pitkänen, A., & Kemppainen, S. (2002). Comparison of the distribution of calcium-binding proteins and intrinsic connectivity in the lateral nucleus of the rat, monkey, and human amygdala. *Pharmacology Biochemistry and Behavior*, *71*(3), 369–377. https://doi.org/10.1016/S0091-3057(01)00690-6

Plesa-Skwerer, D., Faja, S., Schofield, C., Verbalis, A., & Tager-Flusberg, H. (2006). Perceiving facial and vocal expressions of emotion in individuals with Williams syndrome. *American Journal of Mental Retardation : AJMR*, *111*(1), 15–26. https://doi.org/10.1352/0895-8017(2006)111[15:PFAVEO]2.0.CO;2

Plesa-Skwerer, D., Ammerman, E., André, M.-C., Ciciolla, L., Fine, A. B., & Tager-Flusberg, H. (2011). A multimeasure approach to investigating affective appraisal of social information in Williams syndrome. *Journal of Neurodevelopmental Disorders*, *3*(4), 325–334. https://doi.org/10.1007/s11689-011-9100-9

Pober, B. R. (2010). Williams–Beuren Syndrome. *New England Journal of Medicine*, *362*(3), 239–252. https://doi.org/10.1056/NEJMra0903074

Porter, M. A., Dobson-Stone, C., Kwok, J. B. J., Schofield, P. R., Beckett, W., & Tassabehji, M. (2012). A Role for Transcription Factor GTF2IRD2 in Executive Function in Williams-Beuren Syndrome. *PLoS ONE*, *7*(10), e47457. https://doi.org/10.1371/journal.pone.0047457

Prager, E. M., Bergstrom, H. C., Wynn, G. H., & Braga, M. F. M. (2016). The basolateral amygdala γ-aminobutyric acidergic system in health and disease. *Journal of Neuroscience Research*, *94*(6), 548–567. https://doi.org/10.1002/jnr.23690

Price, J. L., & Amaral, D. G. (1981). An autoradiographic study of the projections of the central nucleus of the monkey amygdala. *The Journal of Neuroscience : The Official Journal of the Society for Neuroscience*, *1*(11), 1242–1259. https://doi.org/10.1523/JNEUROSCI.01-11-01242.1981

Rainnie, D. G., Mania, I., Mascagni, F., & McDonald, A. J. (2006). Physiological and morphological characterization of parvalbumin-containing interneurons of the rat basolateral amygdala. *The Journal of Comparative Neurology*, *498*(1), 142–161. https://doi.org/10.1002/cne.21049

Reiss, A L, Eliez, S., Schmitt, J. E., Straus, E., Lai, Z., Jones, W., & Bellugi, U. (2000). IV. Neuroanatomy of Williams syndrome: a high-resolution MRI study. *Journal of Cognitive Neuroscience*, *12 Suppl 1*, 65–73. Retrieved from http://www.ncbi.nlm.nih.gov/pubmed/10953234

Reiss, Allan L, Eckert, M. A., Rose, F. E., Karchemskiy, A., Kesler, S., Chang, M., Reynolds, M.F., Kwon, H., & Galaburda, A. (2004). An experiment of nature: brain anatomy parallels cognition and behavior in Williams syndrome. *The Journal of Neuroscience : The Official Journal of the Society for Neuroscience*, *24*(21), 5009–5015. https://doi.org/10.1523/JNEUROSCI.5272-03.2004

Rodrigues, S. M., Schafe, G. E., & LeDoux, J. E. (2004). Molecular Mechanisms Underlying Emotional Learning and Memory in the Lateral Amygdala. *Neuron*, *44*(1), 75–91. https://doi.org/10.1016/J.NEURON.2004.09.014

Sadakata, T., Washida, M., Iwayama, Y., Shoji, S., Sato, Y., Ohkura, T., Katoh-Semba, R., Nakajima, M., Sekine, Y., Tanaka, M., Nakamura, K., Iwata, Y., Tsuchiya, K. J., Mori, N., Detera-Wadleigh, S. D., Ichikawa, H., Itohara, S., Yoshikawa, T., & Furuichi, T. (2007). Autistic-like phenotypes in Cadps2-knockout mice and aberrant CADPS2 splicing in autistic patients. *The Journal of Clinical Investigation*, *117*(4), 931–943. https://doi.org/10.1172/JCI29031

Sah, P., Faber, E. S. L., Lopez de Armentia, M., & Power, J. (2003). The Amygdaloid Complex: Anatomy and Physiology. *Physiological Reviews*, *83*(3), 803–834. https://doi.org/10.1152/physrev.00002.2003

Sanders, S. J., Ercan-Sencicek, A. G., Hus, V., Luo, R., Murtha, M. T., Moreno-De-Luca, D., Chu, S. H., Moreau, M. P., Gupta, A. R., Thomson, S. A., Mason, C. E., Bilguvar, K., Celestino-Soper, P. B., Choi, M., Crawford, E. L., Davis, L., Wright, N. R., Dhodapkar, R. M., DiCola, M., DiLullo, N. M., Fernandez, T. V., Fielding-Singh, V., Fishman, D. O., Frahm, S., Garagaloyan, R., Goh, G. S., Kammela, S., Klei, L., Lowe, J. K., Lund, S. C., McGrew, A. D., Meyer, K. A., Moffat, W. J., Murdoch, J. D., O'Roak, B. J., Ober, G. T., Pottenger, R. S., Raubeson, M. J., Song, Y., Wang, Q., Yaspan, B. L., Yu, T. W., Yurkiewicz, I. R., Beaudet, A. L., Cantor, R. M., Curland, M., Grice, D. E., Günel, M., Lifton, R. P., Mane, S. M., Martin, D. M., Shaw, C. A., Sheldon, M., Tischfield, J. A., Walsh, C. A., Morrow, E. M., Ledbetter, D. H., Fombonne, E., Lord, C., Martin, C. L., Brooks, A. I., Sutcliffe, J. S., Cook, E. H. Jr., Geschwind, D., Roeder, K., Devlin, B., & State, M. W. (2011). Multiple recurrent de novo CNVs, including duplications of the 7q11.23 Williams syndrome region, are strongly associated with autism. *Neuron*, *70*(5), 863–885. https://doi.org/10.1016/j.neuron.2011.05.002

Schumann, C. M., Bauman, M. D., & Amaral, D. G. (2011). Abnormal structure or function of

the amygdala is a common component of neurodevelopmental disorders. *Neuropsychologia*, *49*(4), 745–759. https://doi.org/10.1016/j.neuropsychologia.2010.09.028

Schumann, C. M., & Amaral, D. G. (2006). Stereological Analysis of Amygdala Neuron Number in Autism. *The Journal of Neuroscience*, *26*(29), 7674–7679. https://doi.org/10.1523/JNEUROSCI.1285-06.2006

Schumann, C. M., Hamstra, J., Goodlin-Jones, B. L., Lotspeich, L. J., Kwon, H., Buonocore, M. H., Lammers, C. R., Reiss, A. L., & Amaral, D. G. (2004). The Amygdala Is Enlarged in Children But Not Adolescents with Autism; the Hippocampus Is Enlarged at All Ages. *The Journal of Neuroscience*, *24*(28), 6392–6401. https://doi.org/10.1523/JNEUROSCI.1297-04.2004

Selby, L., Zhang, C., & Sun, Q.-Q. (2007). Major defects in neocortical GABAergic inhibitory circuits in mice lacking the fragile X mental retardation protein. *Neuroscience Letters*, *412*(3), 227–232. https://doi.org/10.1016/j.neulet.2006.11.062

Semmler, A., Frisch, C., Debeir, T., Ramanathan, M., Okulla, T., Klockgether, T., & Heneka, M. T. (2007). Long-term cognitive impairment, neuronal loss and reduced cortical cholinergic innervation after recovery from sepsis in a rodent model. *Experimental Neurology*, *204*(2), 733–740. https://doi.org/10.1016/J.EXPNEUROL.2007.01.003

Serrano-Juárez, C. A., Venegas-Vega, C. A., Yáñez-Téllez, M. G., Rodríguez-Camacho, M., Silva-Pereyra, J., Salgado-Ceballos, H., & Prieto-Corona, B. (2018). Cognitive, Behavioral, and Adaptive Profiles in Williams Syndrome With and Without Loss of GTF2IRD2. *Journal of the International Neuropsychological Society*, *24*(09), 896–904. https://doi.org/10.1017/S1355617718000711

Siami, S., Annane, D., & Sharshar, T. (2008). The Encephalopathy in Sepsis. *Critical Care Clinics*, *24*(1), 67–82. https://doi.org/10.1016/J.CCC.2007.10.001

Sorvari, H., Miettinen, R., Soininen, H., & Pitkänen, A. (1996). Parvalbumin-immunoreactive neurons make inhibitory synapses on pyramidal cells in the human amygdala: a light and electron microscopic study. *Neuroscience Letters*, *217*(2–3), 93–96. https://doi.org/10.1016/0304-3940(96)13067-6

Sorvari, H., Soininen, H., Paljärvi, L., Karkola, K., & Pitkänen, A. (1995). Distribution of parvalbumin-immunoreactive cells and fibers in the human amygdaloid complex. *The Journal of Comparative Neurology*, *360*(2), 185–212. https://doi.org/10.1002/cne.903600202

Spampanato, J., Polepalli, J., & Sah, P. (2011). Interneurons in the basolateral amygdala. *Neuropharmacology*, *60*(5), 765–773. https://doi.org/10.1016/J.NEUROPHARM.2010.11.006

Stearns, N. A., Schaevitz, L. R., Bowling, H., Nag, N., Berger, U. V., & Berger-Sweeney, J. (2007). Behavioral and anatomical abnormalities in Mecp2 mutant mice: A model for Rett syndrome. *Neuroscience*, *146*(3), 907–921.

https://doi.org/10.1016/J.NEUROSCIENCE.2007.02.009

Stefanacci, L., & Amaral, D. G. (2000). Topographic organization of cortical inputs to the lateral nucleus of the macaque monkey amygdala: A retrograde tracing study. *The Journal of Comparative Neurology*, *421*(1), 52–79. https://doi.org/10.1002/(SICI)1096-9861(20000522)421:1<52::AID-CNE4>3.0.CO;2-O

Stefanacci, L., & Amaral, D. G. (2002). Some observations on cortical inputs to the macaque monkey amygdala: An anterograde tracing study. *The Journal of Comparative Neurology*, *451*(4), 301–323. https://doi.org/10.1002/cne.10339

Stefanacci, L., Suzuki, W. A., & Amaral, D. G. (1996). Organization of connections between the amygdaloid complex and the perirhinal and parahippocampal cortices in macaque monkeys. *The Journal of Comparative Neurology*, *375*(4), 552–582. https://doi.org/10.1002/(SICI)1096-9861(19961125)375:4<552::AID-CNE2>3.0.CO;2-0

Strømme, P., Bjømstad, P. G., & Ramstad, K. (2002). Prevalence Estimation of Williams Syndrome. *Journal of Child Neurology*, *17*(4), 269–271. https://doi.org/10.1177/088307380201700406

van Hagen, J. M., van der Geest, J. N., van der Giessen, R. S., Lagers-van Haselen, G. C., Eussen, H. J. F. M. M., Gille, J. J. P., Govaerts, L. C., Wouters, C. H., de Coo, I. F., Hoogenraad, C. C., Koekkoek, S. K., Frens, M. A., van Camp, N., van der Linden, A., Jansweijer, M. C., Thorgeirsson, S. S., & De Zeeuw, C. I. (2007). Contribution of CYLN2 and GTF2IRD1 to neurological and cognitive symptoms in Williams Syndrome. *Neurobiology of Disease*, *26*(1), 112–124. https://doi.org/10.1016/j.nbd.2006.12.009

Vislay, R. L., Martin, B. S., Olmos-Serrano, J. L., Kratovac, S., Nelson, D. L., Corbin, J. G., & Huntsman, M. M. (2013). Homeostatic responses fail to correct defective amygdala inhibitory circuit maturation in fragile X syndrome. *The Journal of Neuroscience : The Official Journal of the Society for Neuroscience*, *33*(17), 7548–7558. https://doi.org/10.1523/JNEUROSCI.2764-12.2013

Vivanti, G., Hamner, T., & Lee, N. R. (2018). Neurodevelopmental Disorders Affecting Sociability: Recent Research Advances and Future Directions in Autism Spectrum Disorder and Williams Syndrome. *Current Neurology and Neuroscience Reports*, *18*(12), 94. https://doi.org/10.1007/s11910-018-0902-y

Volk, D. W., & Lewis, D. A. (2015). Schizophrenia. *Rosenberg's Molecular and Genetic Basis of Neurological and Psychiatric Disease*, 1293–1299. https://doi.org/10.1016/B978-0-12-410529-4.00105-4

Wessel, A., Pankau, R., Kececioglu, D., Ruschewski, W., & Bürsch, J. H. (1994). Three decades of follow-up of aortic and pulmonary vascular lesions in the Williams-Beuren syndrome. *American Journal of Medical Genetics*, *52*(3), 297–301. https://doi.org/10.1002/ajmg.1320520309

Woo, T. U., Whitehead, R. E., Melchitzky, D. S., & Lewis, D. A. (1998). A subclass of

prefrontal gamma-aminobutyric acid axon terminals are selectively altered in schizophrenia. *Proceedings of the National Academy of Sciences of the United States of America*, *95*(9), 5341–5346. https://doi.org/10.1073/PNAS.95.9.5341

Woodruff, A. R., Monyer, H., & Sah, P. (2006). GABAergic excitation in the basolateral amygdala. *The Journal of Neuroscience : The Official Journal of the Society for Neuroscience*, *26*(46), 11881–11887. https://doi.org/10.1523/JNEUROSCI.3389-06.2006

Woodruff, A. R., & Sah, P. (2007a). Inhibition and Synchronization of Basal Amygdala Principal Neuron Spiking by Parvalbumin-Positive Interneurons Neural circuits for fear renewal View project Non-genomic actions of vitamin D within the developing brain View project. *Article in Journal of Neurophysiology*. https://doi.org/10.1152/jn.00739.2007

Woodruff, A. R., & Sah, P. (2007b). Networks of parvalbumin-positive interneurons in the basolateral amygdala. *The Journal of Neuroscience : The Official Journal of the Society for Neuroscience*, *27*(3), 553–563. https://doi.org/10.1523/JNEUROSCI.3686-06.2007

Young, E. J., Lipina, T., Tam, E., Mandel, A., Clapcote, S. J., Bechard, A. R., Chambers, J., Mount, H. T., Fletcher, P. J., Roder, J. C., & Osborne, L. R. (2008). Reduced fear and aggression and altered serotonin metabolism in Gtf2ird1-targeted mice. *Genes, Brain, and Behavior*, *7*(2), 224–234. https://doi.org/10.1111/j.1601-183X.2007.00343.x